TabKDE: Simple and Scalable Tabular Data Generation with Kernel Density Estimates

Anonymous authors
Paper under double-blind review

Abstract

Tabular data generation considers a large table with multiple columns – each column comprised of numerical, categorical, or sometimes ordinal values. The goal is to produce new rows for the table that replicate the distribution of rows from the original data – without just copying those initial rows. The last 3 years have seen enormous progress on this problem, mostly using computational expensive methods that employ one-hot encoding, VAEs, and diffusion.

This paper describes a new approach to the problem of tabular data generation. By employing copula transformations and modeling the distribution as a kernel density estimate we can nearly match the accuracy and privacy-preservation achievements of the previous methods, but with almost no training time. Our method is very scalable, and can be run on data sets orders of magnitude larger than prior state-of-the-art on a simple laptop. Moreover, because we employ kernel density estimates, we can store the model as a coreset of the original data – we believe the first for generative modeling – and as a result, require significantly less space as well. Our code is available here: `http://github.com/tabkde/tabkde-main`

1 Introduction

Tabular data is a fundamental format in many domains, including finance, healthcare, and social sciences, and has seen much recent attention (Fonseca & Bacao, 2023; Assefa et al., 2021; Hernandez et al., 2022; Ouyang et al., 2023), focusing on challenges in scalability and accuracy in its diverse structural characteristics (Xu et al., 2019; Borisov et al., 2023; Liu et al., 2023). Unlike image or text data, which follow well-defined spatial or sequential relationships, tabular data consists of mixture of varied features that may be numerical, categorical, or ordinal. This heterogeneity poses difficulties in modeling feature dependencies and joint distributions effectively. Traditional generative approaches, such as GANs and VAEs, have been applied with mixed success, and may need to be paired with careful preprocessing and one-hot encoding, which can lead to an explosion in dimensionality and loss of information (Xu et al., 2019; Zhang et al., 2024). Moreover, adversarial training in GANs can be unstable (Arjovsky & Bottou, 2017), while VAEs may struggle to generate realistic samples due to overly simplistic latent space assumptions (Dai & Wipf, 2019).

Copula-based data generators (Patki et al., 2016; Majdara & Nooshabadi, 2020) provide another approach towards transforming differently structured and scaled columns into common format. The synthetic data vault (SDV) (Patki et al., 2016) includes generative modeling through a variety of approaches including low-rank modeling, GANs, and vine-copula (Meyer et al., 2021). This framework can achieve improved fidelity, but sometimes at a heavy computational expense.

Diffusion models have recently emerged as powerful generative frameworks, demonstrating impressive performance in domains such as image synthesis and molecular generation (Ho et al., 2020; Rombach et al., 2022; Dhariwal & Nichol, 2021; Morehead & Cheng, 2024; Luo et al., 2024). These models operate by progressively transforming noise into structured data through a learned denoising process. Recent advances, such as TabDDPM (Kotelnikov et al., 2023), TabSYN (Zhang et al., 2024), and TabDiff (Shi et al., 2025) have made significant progress in adapting diffusion to the tabular setting. TabDDPM (Kotelnikov et al., 2023) applies a diffusion model directly to tabular data, effectively capturing complex distributions but requiring a

high number of sampling steps. TabSYN (Zhang et al., 2024) introduced a latent-space diffusion approach (similar to stable diffusion model approach (Rombach et al., 2022)): it first encodes categorical features with a one-hot encoding, then invokes a VAE to map to a structured representation before applying a diffusion model. This approach has demonstrated remarkable improvements in synthetic data quality, outperforming previous methods in terms of statistical fidelity. TabDiff (Shi et al., 2025) extends this by applying a discrete state-space diffusion for the categorical features.

Challenges with the synthetic tabular data generation. Ultimately, effective tabular data generation needs to overcome three challenges. First, it should achieve **high accuracy** in how the distribution of data it generates aligns with heldout data along marginal, pairwise correlations, and full joint distributional measurements. Most prior methods without diffusion are not able to hit high levels of accuracy. Second, it should **preserve privacy** of the test data; it cannot just generate synthetic data too similar to the data it was trained on. For instance, smote (Chawla et al., 2002) while successful in other metrics, often re-generates training data, or very close to it. Third, it should be **scalable and efficient**; that is, it should be able to easily handle very large training sets, and – more challengingly – data with many categories. Methods based on one-hot encoding like TabSYN can run out of memory with large numbers of categories, and diffusion-based approaches can be relatively slow to train. *No prior method achieves all three desiderata*; see Table 1.

1.1 Our Contribution

We propose a new approach to tabular data generation, TabKDE, that achieves all three desiderata; see Table 1. Notably, it only uses classic tools (carefully assembled): copula transformation, covariance estimation, kernel density estimation. We argue this simplicity improves the interpretability, and we demonstrate (in Section 3) that while nearly-matching SOTA accuracy and privacy it significantly reduces the computational cost in training and generation. It has the following specific advantages.

- **Scalability.** It is more scalable and efficient than methods (like TABDDPM (Kotelnikov et al., 2023) and TabSYN (Zhang et al., 2024)) which rely on one-hot encoding and need to train an expensive diffusion model. These falter by running out of memory on datasets with many categories.
- **Preserving Privacy.** TabKDE preserves privacy while not requiring extensive training. In contrast smote (Chawla et al., 2002), which also does not have a training step, often generates data too close to the data it was trained on.
- **Coreset for Tabular Data Generation.** For the first time, we construct a coreset for tabular data generation. By mapping data into a space where kernel density estimates are applicable, we can apply coresets for KDEs which compactly (and sub-linearly in training size) represents the generative process.

To better contextualize Table 1, note that low-fidelity generators can misleadingly shift results in favor of DCR, creating the illusion of strong privacy, simply because their synthetic data deviates sharply from the real distribution. For example, CoDi and STaSy exhibit substantially larger marginal and pairwise errors, as well as markedly lower C2ST scores than TabSYN and TabKDE (see Tables 17, 19, and 24), underscoring their poor accuracy. Their apparent DCR advantage (Table 27) thus reflects this low fidelity rather than genuinely stronger privacy.

Overview of our approach: TabKDE. We follow the general three step paradigm of (Rombach et al., 2022), applied to tabular data. **(1) Encoding** converts the input into a standardized continuous representation. After this step each of categorical, ordinal, and numerical features are then represented in the same continuous format. **(2) Embedding into a Distance-Aware Latent Space** uses a continuous mapping into another continuous space where now Euclidean distance between objects is representative of how similar they are. **(3) Generative Modeling** maps the discrete distribution of training data in the latent space to a continuous distribution from which we can sample from. The samples are then made in the latent space, inverted to the encoded format, and decoded to be in the format of the input table.

Table 1: Comparison of popular tabular data synthesis methods across key criteria.

Method	citation	Scalable	Accurate	Private
SMOTE	(Chawla et al., 2002)	✓	✓	x
GReaT	(Borisov et al., 2023)	x	x	x
GOGGLE	(Liu et al., 2023)	x	x	x
CoDi	(Lee et al., 2023)	x	x	x
STaSy	(Kim et al., 2023)	x	x	x
TabDDPM	(Kotelnikov et al., 2023)	x	✓	✓
TabSYN	(Zhang et al., 2024)	x	✓	✓
CoreTabKDE	coreset variant	✓	✓	✓
TabKDE	main contribution	✓	✓	✓

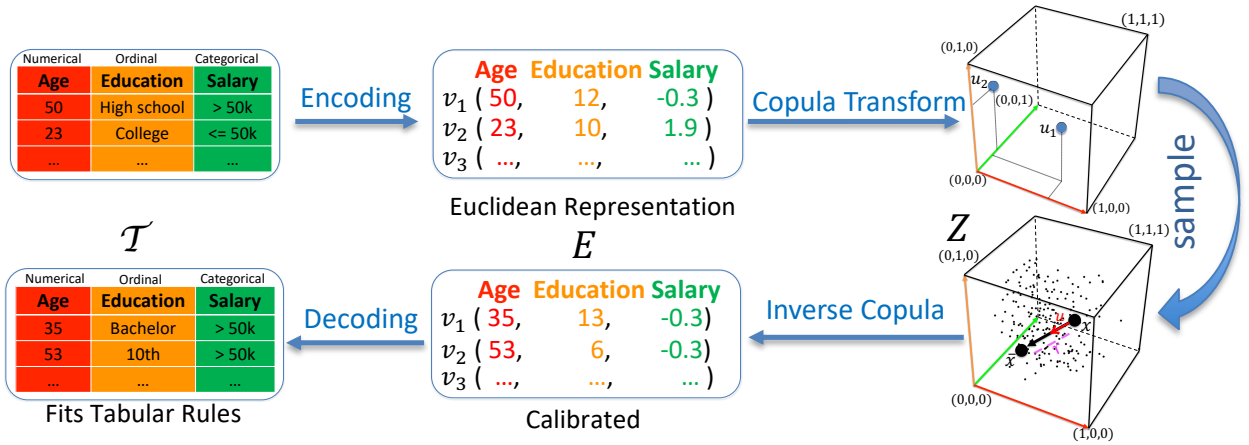

Figure 1: An overview of the proposed TabKDE.

Figure 1 illustrates how we implement the general framework; notably we avoid one-hot encoding (which can blow up memory requirements), VAEs and diffusion (which can be slow to train), to achieve a scalable method which can still achieve high accuracy and retain privacy.

Our method TabKDE first converts all features—numerical, ordinal, and categorical—into a unified numerical format; importantly, it does so in a careful way, so each column in the table is represented as a single numerical value. This is followed by a copula-based transformation that maps the data into a unit hypercube for easier (marginal) density estimation. Here its covariance is also calibrated. Then the generative process uses Kernel Density Estimation (KDE) modeling to represent and sample from a distribution. The only training is in learning the shape of the kernel to match the distance to closest record. Note that sampling from a KDE is simple, in that it needs only to choose a data point, a (covariance scaled) direction, and an offset distance. Then generated samples are mapped back by inverting the copula transform, and decoded. One key additional step is performed to ensure all samples are within the margins identified by the copula, otherwise partial resampling is performed.

2 TabKDE Algorithm

We consider a tabular dataset $\mathcal{T} = \{X_1, X_2, \ldots, X_m\}$, where each row X_i represents an independent and identically distributed (i.i.d.) sample from an unknown joint distribution $P(X)$. Each row $X_i = (x_1, x_2, \ldots, x_d)$ is a d-dimensional vector where each feature x_j belongs to one of three categories: Numerical (Num), Ordinal (Ord), and Categorical (Cat). Each numerical is in $\mathbb{R}$, but both categorical and ordinal features come from a discrete domain; the difference being that ordinal features have a specified ordering (e.g., grades $A > B > C$).

The *key innovation* of TabKDE is in the careful combination of copula mapping to latent space and the KDE-based generative modeling approach.

Copula Latent Space Mapping: It uses a copula-based transformation of the tabular dataset $\mathcal{T}$ into a latent representation Z that lies within the continuous $[0,1]^d$, allowing precise control over the domain of the marginal distributions. This dimension and margin preservation critically leverages principal vector guided encoding of categorical features. Then the covariance Σ of data in this space allows for modeling the directional variation of the data within these bounds.

KDE Generative Modeling: Here we use a KDE model to allow for a non-parametric complex distributional model. We simply sample by choosing a training data point in the latent space $z \sim \mathsf{Unif}(Z)$, and then choose a random direction u proportional to the covariance Σ. Then generate:

$$z' \leftarrow z + ur$$

where r is a scalar controlling the amount of deviation from the training data. In particular, we select r at random from a learned distribution from the training data estimating the distance to the closest point. One more idea is needed, we disallow points outside $[0,1]^d$ to respect the original column marginals. To handle this, we keep coordinates within $[0,1]^d$, and regenerate the others iteratively.

Pipeline overview. Putting the pieces together, TabKDE proceeds as follows:

1. Encode each table row into a d-dimensional numeric representation E with one scalar per original column (Section 2.1);
2. Apply a per-coordinate copula transform (empirical CDF) to map into a bounded latent space $Z \subset [0,1]^d$ that preserves marginal support and is invertible (Section 2.2);
3. Compute the latent covariance Σ and estimate a distance-to-closest-record radius distribution f in this copula space (Section 2.3);
4. Now we can generate a latent sample by choosing a seed point $z_i \in Z$, drawing a covariance-aligned direction u, drawing a radius $r \sim f$, proposing $z' = z_i + ru$, enforcing $z' \in [0,1]^d$ via boundary-aware resampling, and finally decoding back to the original tabular domain via the inverse copula map (Section 2.4).

2.1 Encoding of Tabular Features: $\mathcal{T} \to E$

For tabular data $\mathcal{T} = \{X_1, \ldots, X_n\}$ with d coordinates, we first encode each row X_i into a space $E \subset \mathbb{R}^d$. Importantly the space E has one dimension for each column in $\mathcal{T}$. Numerical values are left as they are, and ordinal values are assigned values $1, 2, 3, \ldots$ for the rank of the ordinal category.

For categorical data we avoid one-hot encoding, and instead apply PrincipalGuidedEncoding (PGE). It first computes a vector $v \in \mathbb{R}^{d'}$, the top principal vector of the $d' \leq d$ numerical features matrix $Z \in \mathbb{R}^{n \times d_1}$ (z-score normalized); this captures the largest mode of variation among the numerical data. It then performs a one-dimensional reduction by projecting Z onto this top principal direction v, yielding $u = Zv \in \mathbb{R}^n$, where u denotes the *first principal component scores* (PC1 scores). Then for each categorical dimension $j \in \mathsf{Cat}$ with category set C_j, it uses u to numerically encode each category. That is, for each category $c \in C_j$ it considers all row indices whose jth coordinate equals c; call this set $I_{j,c} = \{i \in [n] \mid (X_i)_j = c\}$. Then it assigns the category c the average first principal component score among those rows; that is

$$v_{j,c} = \frac{1}{|I_{j,c}|} \sum_{i \in I_{j,c}} u_i.$$

The discrete category c is replaced with that average value $v_{j,c}$ in the space E. Intuitively, this uses the first principal component scores as a one-dimensional "ruler": categories that co-occur with similar numerical profiles tend to receive nearby codes, enabling a single-coordinate representation that can preserve cat–num structure without increasing dimensionality. These categorical dimension can be detokenized by randomly rounding to one of the two nearest values proportional to how close it is. Additional diagnostics and ablation

studies for PGE are provided in Section 3.2, where we compare it against standard scalar encodings that map each categorical value to a single number.

To the best of our knowledge, this is a new method in this context of generative modeling of tabular data, but is also folklore with similar ideas appearing in applied work (c.f. (Saukani & Ismail, 2019)).

2.2 Map to Numerical Latent Space: $E \to Z$

Next we map to a latent space Z where the distances measure closeness between objects. Our representation will have two aspects. First we will ensure $Z = [0,1]^d$, so each coordinate is continuous value between 0 and 1. We do this with a copula transform (Patki et al., 2016) where among the encoded training data $E_i \in E$, each coordinate $E_{i,j}$ is assigned its value in the empirical CDF. So $Z_{i,j}$ is the fraction of $E_{i',j} \leq E_{i,j}$. We store the sorted order of the values $E_{i,j}$ so we can invert this.

Second, after have built Z via a copula map in each coordinate, we then compute sample covariance Σ of Z. This induces a Mahalanobis distance, and Σ will be important for generative sampling.

2.3 Learning Distance to Closest Record (DCR)

In generative sampling, one often computes the *distance to closest record (DCR)* (Mateo-Sanz et al., 2004; Steier et al., 2025) to evaluate how similar a synthetic record s is to a real one from a set Z.

$$\mathrm{DCR}(s, Z) = \min_{z \in Z} \|s - z\|$$

A DCR of 0 may indicate an identical match, posing a significant privacy risk. We can compare DCR values from synthetic data to both training Z_T and holdout Z_H datasets. Ideally, for synthetic data S, DCR distributions $\{\mathrm{DCR}(s, Z_T)\}_{s \in S}$ and $\{\mathrm{DCR}(s, Z_H)\}_{s \in S}$ should heavily overlap, showing that synthetic data reflects general patterns rather than replicating specific records.

As part of our generative process, we learn this distribution $\{\mathrm{DCR}(s, Z)\}_{s \in S}$ where Z is the training data in the copula space. Then we can generate synthetic data to mirror this scale of variation. We repeatedly randomly split the training data, and compute the DCR distribution between the two splits. Then we fit a simple mixture of k Gaussians f to this distribution; choosing k (from $1, \ldots, 10$) using Bayesian Information Criterion. We use the learned DCR distribution f as the perturbation-radius prior in the KDE sampler (Alg. 2). Estimating f by computing DCRs between two random halves of the training set yields an empirical model of the nearest-neighbor spacing expected from independent draws from the same underlying data distribution at finite sample size. Drawing radii $r \sim f$ therefore calibrates the typical displacement of a synthetic point from its seed z_i: radii that are too small tend to collapse toward memorization (unusually low DCR to training points), whereas radii that are too large push samples out of distribution. By matching this characteristic radius scale, TabKDE can generate high-fidelity samples while avoiding overly close replicas of the training data.

2.4 Tabular Kernel Density Estimation: $Z \to$ Sample

A *kernel density estimation (KDE)* is a continuous estimate of a probability density function built by smoothing finite data samples with a kernel function K (often Gaussian) and bandwidth h. For n data points $X = \{x_1, \ldots, x_n\} \sim P$, if we appropriately adjust h as n grows, then the KDE defined $\mathrm{KDE}_X(x) = \frac{1}{n} \sum_{i=1}^{n} K((x - x_i)/h)$ will converge to P (Silverman, 1986; Scott, 2015). Moreover, we can generate synthetic data (in a manner that approaches the unknown distribution P) by drawing a random point x_i and then adding an offset defined by K and h.

Sampling from KDE with DCR kernel. In our TabKDE method we adapt this sampling from a KDE of the data in a few subtle ways. First, instead of a Gaussian, we use a kernel with offset radius r matching a learned DCR distribution. Second, instead of selecting the offset direction u uniformly, we draw it proportional to the learned covariance Σ. These two modifications are sketched in Algorithm 1 with a single sample in latent space generated via Algorithm 2.

Algorithm 1 SimpleKDE($\mathcal{T}$)

1: $Z \in [0,1]^{n \times d} \Leftarrow$ Copula-Transform($\mathcal{T}$)
2: $\Sigma \leftarrow$ Covariance(Z)
3: Estimate empirical DCR distribution f
4: **for** $i = 1, \ldots, m$:
5: $\quad z'_i =$ SampleKDE(Z, f, Σ)
6: $\quad y_j \leftarrow$ InverseCopula(z'_j)
7: **return** $Y = \{y_1, \ldots, y_m\}$

Algorithm 2 SampleKDE(Z, f, Σ)

1: Uniformly sample $z_i \in Z$
2: Sample radius $r > 0$ from f
3: Sample $v \sim \mathcal{N}(0, \Sigma)$, set $u = \frac{v}{\|v\|}$
4: **return** $z' \leftarrow z_i + r \cdot u$

However, the SimpleKDE algorithm does not explicitly control the support of the marginals, which is critical for tabular data generation. The copula-transformed representation, however, embeds the data within the unit hypercube, which allows us to control how far a perturbed sampled point x can deviate without violating marginal support. We now introduce a more refined rejection-sampling heuristic (Alg. 3: TabKDE) that effectively enforces these boundary constraints.

Algorithm 3 TabKDE($\mathcal{T}$)

1: $Z \in [0,1]^{n \times d} \Leftarrow$ Copula-Transform($\mathcal{T}$)
2: $\Sigma \leftarrow$ Covariance(Z)
3: Estimate empirical DCR distribution f
4: **for** $i = 1, \ldots, m$:
5: $\quad z'_i =$ SampleKDE-iterative(Z, f, Σ)
6: $\quad y_j \leftarrow$ InverseCopula(z'_j)
7: **return** $Y = \{y_1, \ldots, y_m\}$

Algorithm 4 SampleKDE-iterative(Z, f, Σ)

1: Uniformly sample $z_i \in Z$
2: Sample radius $r > 0$ from f
3: Sample $v \sim \mathcal{N}(0, \Sigma)$, set $u = \frac{v}{\|v\|}$
4: $z' \leftarrow z_i + r \cdot u$
5: **While** $\{j : z'_j \notin [0,1]\} \neq \varnothing$:
6: $\quad J \leftarrow \{j : z'_j \notin [0,1]\}$
7: $\quad$ Sample $v' \sim \mathcal{N}(0, \Sigma)$, set $w = \frac{v'}{\|v'\|}$
8: $\quad s \leftarrow \frac{\|(u_k)_{k \in J}\|}{\|(w_k)_{k \in J}\|}$
9: $\quad u_j \leftarrow s \cdot w_j$ for each $j \in J$
10: $\quad z' \leftarrow z_i + r \cdot u$
11: **return** z'

TabKDE differs from SimpleKDE only in line 5, where it uses the boundary-aware SampleKDE-iterative (Alg 4) instead of the simpler SampleKDE. This modified sampler checks for violations of the unit hypercube boundaries and regenerates out-of-bound coordinates. If a valid point cannot be obtained after a fixed number of attempts, the sample is discarded, and the process restarts. This mechanism guarantees that all accepted samples lie within the latent space $[0,1]^d$. Note that a naive KDE perturbation $z' = z_i + ru$ frequently proposes points with some coordinates < 0 or > 1, especially for seeds near the boundary. Simple fixes such as clipping out-of-range coordinates to 0/1 or rejecting and resampling entire proposals can noticeably distort the distribution: clipping creates artificial probability mass at the boundaries and yields visible marginal artifacts (spikes/heavy tails), while full rejection biases samples away from boundary regions and can disrupt correlations. Our boundary aware sampler prevents this by only resampling the offending coordinates until all coordinates lie in $[0,1]^d$, preserving the intended radius scale r and the covariance-aligned geometry on the remaining coordinates. This avoids the boundary accumulation and out-of-support marginal behavior observed in the non-boundary-aware variant (see Appendix G.1 and Figure 14 for an illustrative marginal failure case). Appendix G.2 presents an ablation analysis illustrating how often the boundary aware sampler corrects a sample across different datasets.

2.5 Coresets for Generative Tabular Data Modeling

A *coreset* (Phillips, 2016) is a compact, weighted set of points that provides a close approximation to the full dataset for a specific downstream task. In the context of KDEs, a coreset serves to approximate the full KDE using significantly fewer, strategically chosen, representative points.

Our proposed TabKDE framework employs the full KDE_Z to generate samples from the Copula latent representation $Z \subset [0,1]^{n \times d}$ of the tabular data $\mathcal{T}$. To approximate $\text{KDE}_Z(\cdot)$ using a coreset, we define $\tilde{\text{KDE}}_\Theta(\cdot)$ with Θ comprised of a small set of learnable coreset points $Q = \{q_1, \ldots, q_m\}$ and their corresponding non-

Table 2: Runtime comparison of Tabsyn, TabKDE, and SMOTE models across individual datasets on laptop. The IBM dataset is excluded from the average row.

Dataset	TabSYN				SMOTE	TabKDE	
	VAE Train	Diff. Train	Total Train	Sample	Train+Sample	Train	Sample
Adult	6h 35m 43s	2h 6m 31s	8h 43m 19s	1m 5s	4s	44s	20s
Default	6h 32m 3s	2h 2m 16s	8h 34m 59s	40s	2s	59s	17s
Shoppers	3h 57m 42s	0h 55m 32s	4h 53m 32s	18s	3s	17s	5s
Magic	3h 51m 7s	1h 21m 27s	5h 13m 0s	26s	5s	19s	7s
Beijing	5h 31m 57s	1h 57m 44s	7h 30m 35s	54s	2s	35s	16s
News	14h 34m 15s	2h 8m 59s	16h 44m 11s	57s	4s	6m 2s	54s
Average	**6h 50m 27s**	**1h 45m 24s**	**8h 36m 36s**	**43s**	**3s**	**1m 29s**	**19s**
IBM	OOM	OOM	OOM	OOM	OOM	10m 21s	6m 4s

negative weights $W = \{\omega_1, \ldots, \omega_m\}$, constrained such that $\sum_{i=1}^{m} \omega_i = 1$. The approximated density function is $\widetilde{\text{KDE}}_\Theta(z) = \sum_{i=1}^{m} \omega_i K\left(\frac{z - q_i}{h}\right)$. It is known (Joshi et al., 2011) that a sample $Q \sim Z$ of $m = O((d/\varepsilon^2)\log(1/\delta))$ points, and uniform weights already ensures a strong L_∞ coreset approximation that $\|\text{KDE}_Z - \text{KDE}_Q\|_\infty \leq \varepsilon$ with probability at least $1 - \delta$. This results holds for kernels where the super-level set (function domain points with function value above a threshold) have VC-dimension $O(d)$; that holds for these Gaussian kernels (super-level sets are balls), and by kernels clipped at the $[0, 1]^d$ boundary as we will ultimately use, since that only increases the VC-dimension by $O(d)$.

Moreover, this can be used as a starting point for an optimized coreset, over the locations Q and their weights W to minimize the empirical L_2 via SGD as $\mathbb{E}_{z \sim \mathsf{Unif}([0,1]^d)}\left[\left(\widetilde{\text{KDE}}_\Theta(z) - \text{KDE}_Z(z)\right)^2\right]$. This optimized version can potentially better preserve key distributional features, such as modes, spread, and overall shape. Moreover, because we are not replicating the training data, it can reduce the risk of overfitting to the data or leaking its private attributes. We call this method CoreTabKDE; and RandCoreTabKDE only samples but does not optimize. We use coresets of size $m = 5000$.

3 Experimental Results

Our experiments are conducted on the six tabular datasets from UCI Machine Learning Repository[1] (Adult, Default, Shoppers, Magic, Beijing, News) with between 12K and 49K rows and a mixture of 11 and 48 dimensions, a mixture of mostly numerical and categorical. We also use an IBM dataset[2] which is significantly larger; it has about 176K rows and 14 dimensions, with 5 ordinal ones, and a total of over 37K total categories. See Appendix B.1 for more detail.

Baselines. We compare our proposed TabKDE method with several popular baselines, including SMOTE (Chawla et al., 2002), GReaT (Borisov et al., 2023), CoDi (Lee et al., 2023), TabDDPM (Kotelnikov et al., 2023), TabSYN (Zhang et al., 2024), and TabDiff (Shi et al., 2025); some comparisons and other methods are deferred to Appendix B.2 for space. We also consider several hybrid models that mix elements of TabKDE with the encoding choices. Notably, in CopulaDiff we first use our CopulaMapping to embed data into a latent space, train a diffusion model there. Broader comparisons with other copula-based methods are in Appendix H.

3.1 Scalability and Efficiency

[1] `https://archive.ics.uci.edu/datasets`

[2] https://www.kaggle.com/code/yichenzhang1226/ibm-credit-card-fraud-detection-eda-random-forest

We measure the scalability and efficiency on both the training time, as well as the sample generation time; sample generation measures time for the full synthetic set – the same size as training set. A key motivating factor for generative modeling of tabular data is for making sensitive datasets available for development teams that want to use the build models without worrying about leaking specific datum. Since these models vary based on the source of the data, regions, and time periods relevant for the analysis, there are frequent retraining on different parts of the full sensitive dataset. In this setting, each retraining needs to generate one data set that can be used as proxy.

Table 3: Average GPU timing

Method	Train (s)	Sample (s)
GReaT	17112.4	251.2
CoDi	18487.6	11.8
TabDDPM	2771.4	70.8
TabSYN	1297.8	8.4
TabKDE	39.2	39.0

We first compare against TabSYN and SMOTE on a laptop using only CPU (2021 Apple 14" MacBook Pro; M1 Pro chip). Table 2 shows that the simple SMOTE algorithm is faster than TabKDE, but the training time of TabKDE is orders of magnitude faster than TabSYN (about 90 seconds to about 8.5 hours). Appendix C shows other baselines have run times in the ballpark of TabSYN. Moreover, both TabSYN and SMOTE run out of memory on the IBM data set since they try to one-hot encode 37K categories, while TabKDE still completes in under 20 minutes.

We compare GPU runtime (NVIDIA RTX A5000; 24GB memory; max power 230W) in Table 3 over the average training and sampling time on Adult, Default, Shoppers, and Magic datasets. TabKDE is still orders of magnitude faster in training, and while other methods can improve upon TabKDE (our code not optimized for GPU) in sampling, this cost is dominated by the training time. We note that TabSYN requires 3.5 hours of GPU training and 1 minute for sampling on IBM, whereas TabKDE trains in 8 seconds and takes more than 7 minutes (433 seconds) to sample.

In addition to TabKDE, we consider coreset-based variants (CoreTabKDE and RandCoreTabKDE) that reduce storage and can improve privacy. RandCoreTabKDE has runtime comparable to TabKDE, whereas CoreTabKDE incurs an additional optimization step, requiring approximately 55 minutes of training time on CPU on average across Adult, Default, Shoppers, Magic, and Beijing (see Appendix F.1). While this dominates the Train time in CoreTabKDE, it is still significantly less than TabSYN, which averages over 8 hours on a CPU, as seen in Table 2.

3.2 Accuracy

In this section, we evaluate the quality of the generated synthetic data using three criteria: (1) marginal distribution alignment, (2) pairwise correlation matching, and (3) finally global alignment between synthetic and hold-out distributions is compared by how well a classifier can separate the distributions.

Marginal distribution alignment. When evaluating synthetic tabular data, the marginal distribution alignment score assesses how closely each individual column matches its real-data distribution represented by train data. Following what was done in the TabSYN paper, we calculate the Kolmogorov–Smirnov (KS) distance for numerical attributes in Num and the Total Variation distance for categorical and ordinal attributes in Cat and Ord. Table 4 presents, for each dataset, the average marginal alignment errors across all features for each method.

Figure 2 provides a visual comparison between some representative selected real marginal distributions and those generated by TabSYN (orange) and TabKDE (green) against the real data distributions (blue). We observe that TabKDE and TabSYN visually match the distributions well, both are about the same. In particular, on numerical data TabKDE seems to do better on more uniform distributions whereas TabSYN does better on spiky ones.

Pairwise correlation alignment. We next measure pairwise correlation between columns. For numerical-numerical pairs, we can use standard Pearson correlations. For pairs that involve categorical or ordinal feature (as in Zhang et al. (2024)) we use contingency-table total variation distances. In both metrics, smaller error values indicate that the synthetic table is more faithful to the original data. Table 5 presents, for each dataset, the average pairwise correlation alignment errors across all features for each method. A heatmap visualization of the divergence between the pairwise correlations in the real and synthetic data is presented in

Table 4: Marginal distribution alignment error; lower is better. In parentheses denotes ratio relative to the smallest value. Baseline values, unless stated otherwise, are taken from (Zhang et al., 2024); the remaining scores (our methods) are obtained using their data split.

Method	Adult	Default	Shoppers	Magic	Beijing	News	Average
SMOTE (Our reproduced)	1.63 (2.55)	1.70 (1.49)	2.66 (2.16)	1.37 (1.93)	2.10 (1.62)	5.47 (3.18)	2.49 (1.75)
GReaT	12.12 (18.94)	19.94 (17.49)	14.51 (11.80)	16.16 (22.76)	8.25 (6.35)	–	14.20 (10.00)
CoDi	21.38 (33.41)	15.77 (13.82)	31.84 (25.89)	11.56 (16.28)	16.94 (13.03)	32.27 (18.78)	21.63 (15.23)
TabDDPM	1.75 (2.73)	1.57 (1.38)	2.72 (2.21)	1.01 (1.42)	1.30 (1.00)	78.75 (45.83)	14.52 (10.23)
TabSYN (Our reproduced)	0.64 (1.00)	1.14 (1.00)	1.23 (1.00)	0.98 (1.38)	2.79 (2.15)	1.72 (1.00)	1.42 (1.00)
PGE-TabSyn	11.21 (17.51)	7.66 (6.72)	12.98 (10.55)	1.36 (1.74)	2.65 (2.39)	18.65 (10.84)	9.08 (6.39)
CopulaDiff	2.01 (3.14)	1.47 (1.29)	2.47 (2.01)	0.94 (1.32)	2.13 (1.64)	2.44 (1.42)	1.91 (1.35)
RandCoreTabKDE	1.61 (2.52)	1.76 (1.54)	2.54 (2.07)	1.01 (1.42)	1.70 (1.31)	2.59 (1.51)	1.87 (3.48)
CoreTabKDE	3.63 (5.67)	3.29 (2.89)	3.23 (2.63)	1.08 (1.52)	3.20 (2.46)	2.87 (1.67)	2.88 (2.03)
TabKDE	1.56 (2.44)	1.55 (1.36)	2.44 (1.98)	0.78 (1.1)	1.37 (1.05)	2.52 (1.47)	1.70 (1.2)

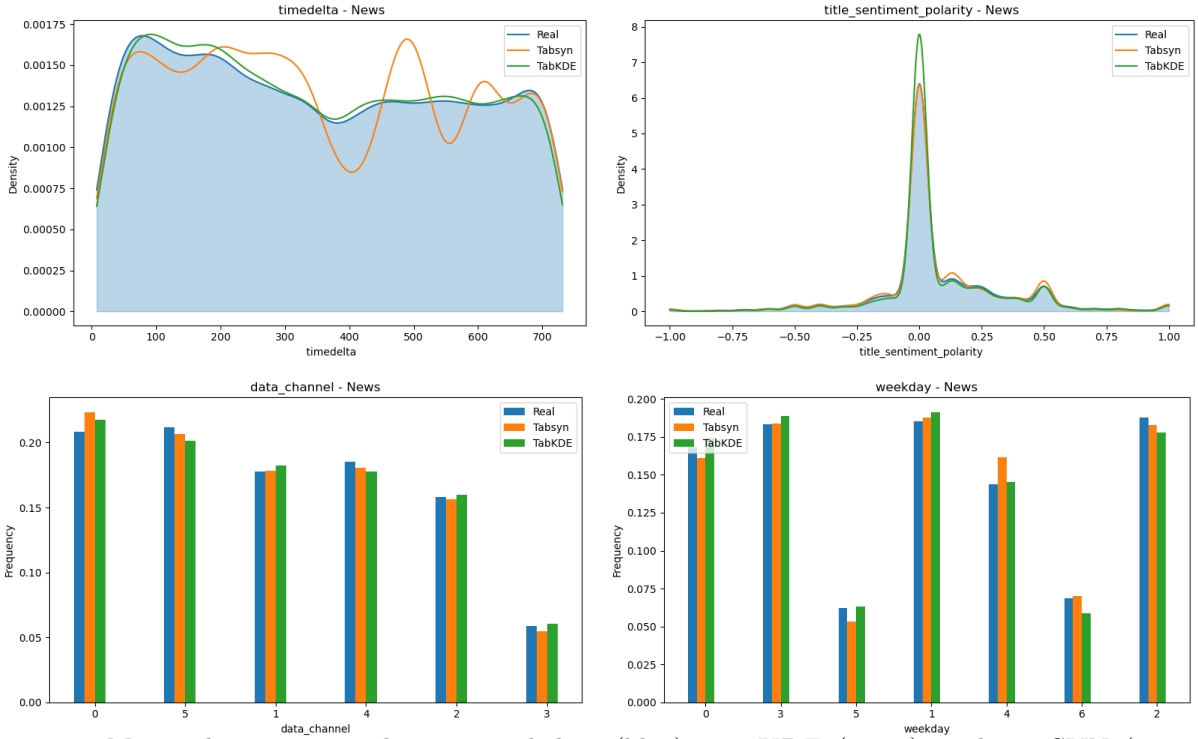

Figure 2: Marginals comparison between real data (blue), TabKDE (green), and TabSYN (orange). Representative numerical and categorical data from News dataset.

Figure 3; see more in Appendix D.2. We observe that TabKDE has better pairwise correlation alignment than all methods except TabSYN, and is comparable to SMOTE; both TabKDE and SMOTE have about 2× the correlation discrepancy as TabSYN.

We also compare against some variants on the larger IBM dataset (See Appendix B.1 for more detail). Recall that on our laptop CPU, neither TabSYN or SMOTE can run on this data set – they both run out of memory. Instead we compare TabKDE against our baselines including CopulaDiff and PGE-TabSyn. Also, note that we apply a modeling trick with Zip / Merchant State / Merchant City and with MCC / Merchant Name with TabKDE but not PGE-TabSyn and TabSYN (on GPU). Recall also that TabKDE (about 10 minutes training time on CPU; 40 seconds on GPU) was much faster than either of CopulaDiff (about 15 hours on CPU), PGE-TabSyn (over 40 hours on CPU) or TabSYN (OOM on CPU, about 20 minutes on GPU). The average pairwise correlation alignment error for TabSYN and PGE-TabSyn (without modeling trick) are 40.42% and 30.53%, respectively, while for TabKDE and CopulaDiff (with modeling trick), are is 25.29% and 22.59%; see Table 6. Indeed as shown in Figure 4 of pairwise correlation plots, the methods work largely

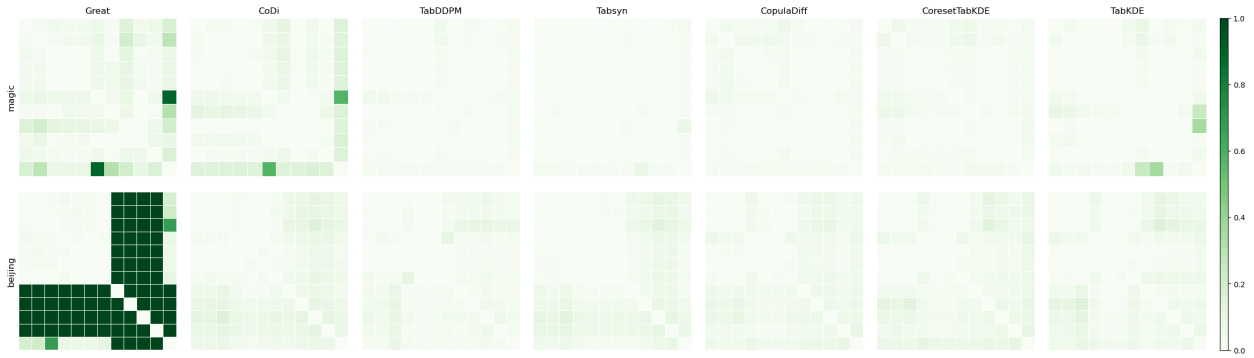

Figure 3: Representative Pairwise correlation divergence heatmaps for Magic and Beijing datasets.

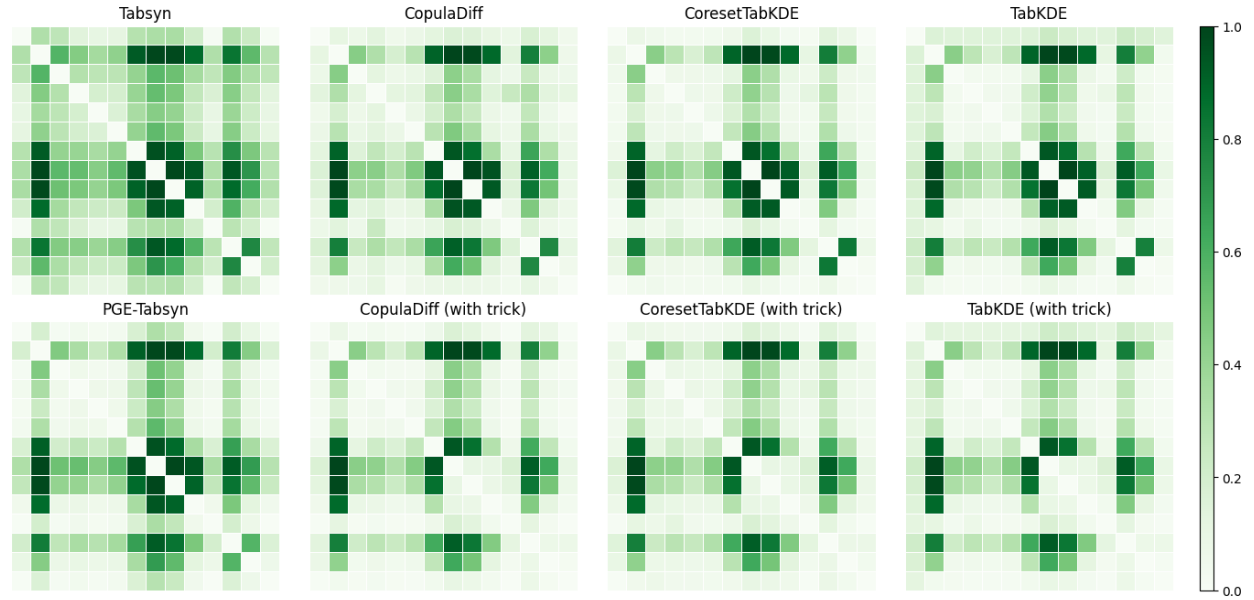

Figure 4: Pairwise correlation Divergence plots for IBM dataset and methods: TabSYN (without modeling trick), PGE-Tabsyn (without modeling trick), CopulaDiff (with and without modeling trick), CoreTabKDE, TabKDE (with and without modeling trick). For CoreTabKDE, the size of coreset and the bandwidth are 5,000 and 0.15, respectively. Models that use the reduced modeling trick are indicated by "with trick" in parentheses.

Table 5: Pairwise correlation alignment error; Lower values is better. In parentheses is the ratio relative to the smallest value. Baseline values, unless stated otherwise, are taken from (Zhang et al., 2024); the remaining scores (our methods) are obtained using their data split.

Method	Adult	Default	Shoppers	Magic	Beijing	News	Average
SMOTE(our reproduction)	4.3 (2.67)	11.54 (5.11)	3.68 (1.47)	1.88 (2.29)	3.3 (1.22)	1.67 (1.25)	4.39 (1.99)
GReaT	17.59 (10.93)	70.02 (30.98)	45.16 (18.06)	10.23 (12.48)	59.6 (21.99)	–	40.52 (18.33)
CoDi	22.49 (13.98)	68.41 (30.27)	17.78 (7.11)	6.53 (7.97)	7.07 (2.61)	11.1 (8.28)	22.23 (10.06)
TabDDPM	3.01 (1.87)	4.89 (2.16)	6.61 (2.64)	1.7 (2.07)	2.71 (1.00)	13.16 (9.82)	5.34 (2.42)
TabSYN (our reproduction)	1.61 (1.00)	2.26 (1.00)	2.5 (1.00)	0.82 (1.00)	4.7 (1.73)	1.34 (1.00)	2.21 (1.00)
PGE-TabSyn	7.14 (4.43)	15.19 (6.72)	7.56 (3.02)	2.67 (2.76)	3.49 (1.29)	4.60 (3.42)	6.78 (3.07)
CopulaDiff	4.61 (2.86)	3.29 (1.46)	5.3 (2.12)	1.72 (2.10)	4.5 (1.66)	2.1 (1.57)	3.59 (1.62)
RandCoreTabKDE	3.93 (2.44)	13.66 (6.04)	4.27 (1.71)	4.76 (5.80)	4.05 (1.49)	2.61 (1.95)	5.46 (2.47)
CoreTabKDE	6.3 (3.91)	9.91 (4.39)	5.77 (2.31)	2.18 (2.66)	5.86 (2.16)	2.82 (2.10)	5.47 (2.48)
TabKDE	4.51 (2.80)	9.93 (4.40)	4.31 (1.72)	2.72 (3.32)	3.74 (1.38)	2.83 (2.11)	4.67 (2.11)

Table 6: Error on IBM. Results below the line have the dimension reduced by a modeling trick to functionally-related coordinates.

Method	Marginal	Pairwise	Reduced
TabSYN	16.99	40.42	no
PGE-TabSyn	9.29	30.53	no
CopulaDiff	6.81	29.42	no
TabKDE	4.36	27.56	no
CopulaDiff	3.59	22.59	yes
CoreTabKDE	5.25	23.93	yes
TabKDE	3.58	25.29	yes

similar except on the highly correlated pairs where we employ the modeling trick. For fairness, we report the results with and without this reduction.

~~We also compare against some variants on the larger IBM dataset in Table 6 and Figure 4. Recall that on our laptop CPU, neither TabSYN or SMOTE can run on this data set – they both run out of memory. For TabKDE we apply a data reduction modeling by first reducing out 3 strongly correlated categories (i.e., state and city depend on zipcode), then inferring them in the decoding step; details in Appendix B.1.~~

Recall also that TabKDE (about 10 minutes training time on CPU; 40 seconds on GPU) was much faster than either of CopulaDiff (about 15 hours on CPU), or TabSYN (OOM on CPU, about 20 minutes on GPU). The average pairwise correlation alignment error for TabSYN (no reduction) is 40.42%, while for TabKDE and CopulaDiff (with reduction) is 25.29% and 22.59%.

Ablation: different categorical encodings. A defining design choice of TabKDE is that the intermediate representation $E \in \mathbb{R}^{n \times d}$ (and thus the copula space $Z \subseteq [0,1]^d$) has *one coordinate per original table column*. This fixed per-column structure makes the copula mapping invertible column-wise and keeps KDE sampling scalable for mixed data types. As a result, TabKDE *must* map each categorical column to a *single real-valued coordinate* (i.e., a continuous code per category) rather than using one-hot expansion. Our default is Principal-Guided Encoding (PGE), though the pipeline is modular: any single-scalar encoding can be substituted, potentially at the cost of fidelity.

To isolate the effect of PGE, we re-run TabKDE and TabSYN with standard single-scalar alternatives, including uniform and frequency-based encodings. Uniform encoding assigns each category a sub-interval of $[0,1]$ with width proportional to its marginal frequency and samples within that interval, yielding an approximately uniform transformed column. Frequency-based encoding also uses only marginal frequencies, but typically maps each category to a fixed scalar derived from its frequency (or a related interval statistic). Tables 7 and 8 report marginal and pairwise alignment errors. We observe that all TabKDE variants perform significantly better (about $1.5 - 1.7$) than TabSYN (about $8.5 - 10$) in marginal error, with still clear but less dramatic improvements in pairwise correlation error. Overall, PGE and Frequency achieve the

lowest average pairwise alignment errors (4.67 and 4.74; Average column of Table 8), indicating the most consistent cross-type fidelity among single-scalar encodings as a key contributor to TabKDE's performance without one-hot expansion. Figure 5 further illustrates correlation divergence for Magic and Beijing via heatmaps, showing how the encoding choice affects the correlation structure. Ultimately, we conclude that Frequency-based encoding could probably replace PGE-encoding without considerable change to the efficacy.

Table 7: Marginal distribution alignment error (lower is better) across different categorical encodings that map each category to a single scalar.

Method	Adult	Default	Shoppers	Magic	Beijing	News	Average
Freq-Tabsyn	12.12	5.53	10.02	1.62	3.82	17.99	8.52
Uni-Tabsyn	10.74	5.56	10.33	1.47	1.40	22.41	8.65
PGE-Tabsyn	11.21	7.66	12.98	1.36	2.65	22.24	9.68
Freq-TabKDE	1.19	1.34	2.52	0.86	1.33	2.49	1.62
Uni-TabKDE	1.58	1.01	2.07	0.75	1.44	2.48	1.56
TabKDE	1.56	1.55	2.44	0.78	1.37	2.52	1.70

Table 8: Pairwise correlation alignment error (lower is better) across different categorical encodings that map each category to a single scalar.

Method	Adult	Default	Shoppers	Magic	Beijing	News	Average
Freq-Tabsyn	11.03	11.66	6.38	3.25	5.76	5.07	7.19
Uni-Tabsyn	9.18	12.48	6.62	3.36	4.10	7.08	7.14
PGE-Tabsyn	7.14	15.19	7.56	2.67	3.49	7.12	7.20
Freq-TabKDE	3.94	10.62	4.05	2.51	4.51	2.80	4.74
Uni-TabKDE	6.28	15.03	4.39	3.65	5.78	2.91	6.34
TabKDE	4.51	9.93	4.31	2.72	3.74	2.83	4.67

Global Distribution Alignment. Synthetic data should be able to take the place of real data, letting us train models on it for downstream prediction tasks and have indistinguishable performance. We assess by building a classifier to attempt to distinguish between the synthetic data and a split of data held out from the training process. We use logistic regression in Table 9 and XGBoost in Appendix D. We quantify this as a classifier two-sample test (C2ST) as provided by SDMetrics; larger values closer to 1 are better.

We observe that TabKDE is roughly the same as SMOTE with 0.93 and only bested by TabSYN which has about 0.97. Other baselines achieve 0.79 (TabDDPM) or below 0.66.

Table 9: C2ST Scores; larger is better. Baseline values, unless stated otherwise, are taken from (Zhang et al., 2024); the remaining scores (our methods) are obtained using their data split.

Method	Adult	Default	Shoppers	Magic	Beijing	News	Average
SMOTE(Our reproduction)	0.9212	0.9332	0.9107	0.9803	0.9972	0.8633	0.9334
GReaT	0.5376	0.4710	0.4285	0.4326	0.6893	—	0.5118
CoDi	0.2077	0.4595	0.2784	0.7206	0.7177	0.0201	0.4007
TabDDPM	0.9755	0.9712	0.8349	0.9998	0.9513	0.0002	0.7888
TabSYN(Our reproduction)	0.9949	0.9804	0.9699	0.9893	0.9268	0.9584	0.9699
PGE-Tabsyn	0.9240	0.9039	0.7679	0.9859	0.8629	0.8060	0.8751
CopulaDiff	0.8557	0.9798	0.8665	0.9914	0.9576	0.9793	0.9384
RandCoreTabKDE	0.9215	0.9570	0.8757	0.9921	0.9503	0.8901	0.9311
CoreTabKDE	0.8254	0.8730	0.8462	0.9864	0.8924	0.8643	0.8813
TabKDE	0.9219	0.9579	0.9161	1.0000	0.9514	0.8819	0.9382

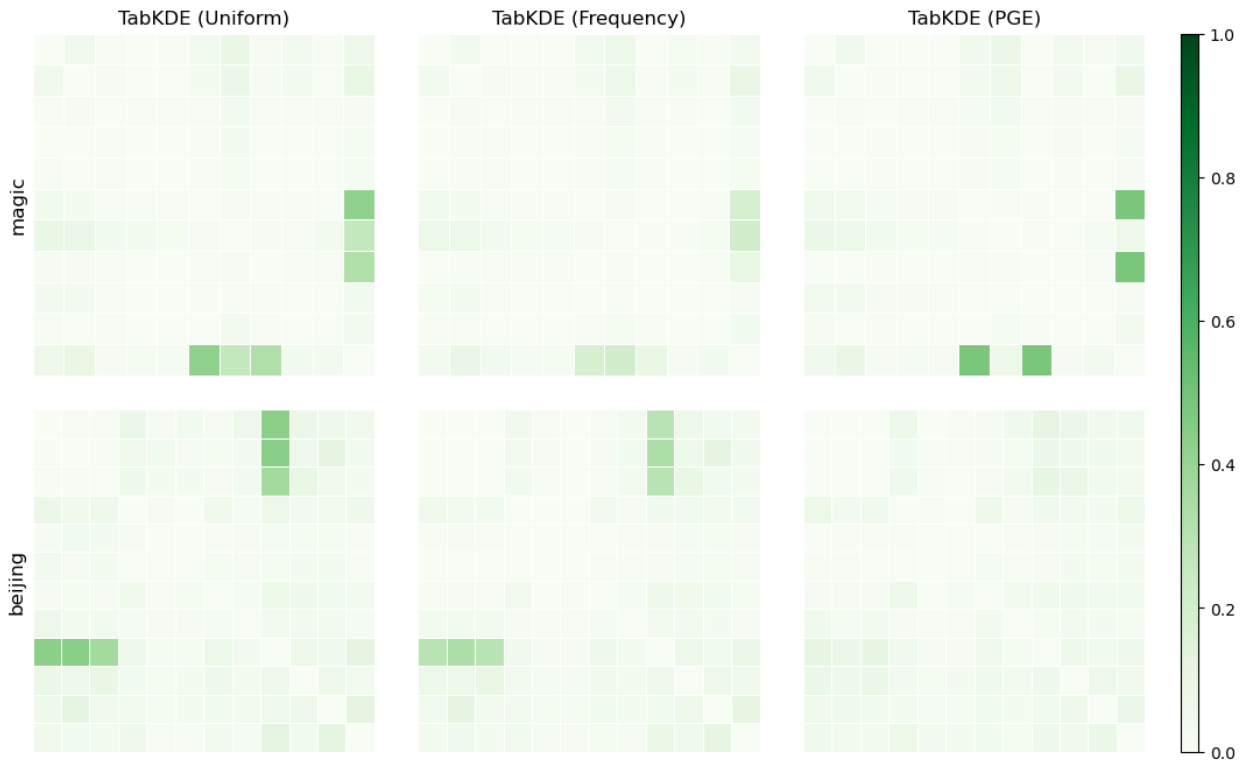

Figure 5: Representative pairwise correlation divergence heatmaps for the Magic and Beijing datasets using TabKDE with different categorical encodings.

Marginal and pairwise statistics do not uniquely determine the joint distribution, and they may miss higher-order dependencies or rare categorical conjunctions. In addition to these metrics and C2ST, we also report *machine learning efficiency* (MLE) (Train-on-Synthetic, Test-on-Real) (Appendix D.3, Table 22), which depends on multi-way feature interactions and therefore serves as an additional higher-order check. We note TabSYN provides the best error, and TabKDE is nearly as good – almost within the natural variation in TabSYN's performance. Perhaps surprisingly, the simple method SMOTE also performs on par with TabSYN and TabKDE.

3.3 Privacy

Finally, we evaluate how well we can preserve the privacy of the training set in synthetic data generation through DCR. For each synthetic data point generated, we compute the distance to training and held-out data. Ideally these distributions should be indistinguishable.

First in Table 10 we calculate the *DCR score*, which is the percentage of synthetic data closer to training data than held-out; we would like this to be close to 50%. This was proposed for TabDiff (Shi et al., 2025), and we show their results in the top half of the table, and also show SMOTE, TabSYN, and our methods following their code below the line. We see most diffusion methods (including our CopulaDiff) can consistently achieve below 52%. Our main method TabKDE obtains an average DCR score of about 58%, which is servicable. SMOTE has an average DCR score of 95% indicating that it reveals significant information (if not replicating) the training data.

The *DCR score is an imperfect measure of privacy*, since there may be heldout data nearly as close as the training data to a synthetic point. Indeed TabKDE is inspired by differential privacy, and the accepted comparison is the ratio of likelihoods, not the count of which one is maximum. So another, albeit less quantitative, evaluation considers the DCR distribution of synthetic data measured to training versus heldout data. Figure 6 shows distribution to training (blue) versus to heldout (red) for representative data on

Table 10: The DCR score for synthetic data sample comparing training to held-out data. A value nearer to 50% is ideal. In parentheses is the ratio relative to the smallest value in each column. Baseline values, unless stated otherwise, are taken from (Zhang et al., 2024); the remaining scores (our methods) are obtained using their data split.

Method	Adult	Default	Shoppers	Beijing	News	Average
SMOTE(Our reproduction)	91.18 (1.83)	91.46 (1.79)	96.76 (1.93)	100.00 (1.99)	99.00 (1.96)	95.68 (1.89)
CoDi	49.92 (1.00)	51.82 (1.02)	51.06 (1.02)	50.87 (1.01)	50.79 (1.01)	50.89 (1.01)
TabDDPM	51.14 (1.02)	52.15 (1.02)	63.23 (1.26)	80.11 (1.59)	79.31 (1.57)	65.19 (1.29)
TabDiff	50.10 (1.00)	51.11 (1.00)	50.24 (1.00)	50.50 (1.00)	51.04 (1.01)	50.60 (1.00)
TabSYN(Our reproduction)	51.33 (1.03)	51.61 (1.01)	51.99 (1.03)	53.20 (1.06)	50.76 (1.01)	51.65 (1.02)
PGE-TabSyn	50.38 (1.01)	51.33 (1.01)	51.81 (1.03)	50.67 (1.01)	50.48 (1.00)	50.94 (1.01)
CopulaDiff	50.34 (1.01)	50.96 (1.00)	50.72 (1.01)	50.29 (1.00)	53.00 (1.05)	51.06 (1.01)
RandCoreTabKDE	62.30 (1.25)	63.09 (1.24)	58.91 (1.17)	63.50 (1.26)	55.59 (1.10)	60.68 (1.20)
CoreTabKDE	52.59 (1.05)	54.11 (1.06)	55.04 (1.10)	51.17 (1.02)	52.00 (1.03)	52.98 (1.05)
TabKDE	62.23 (1.25)	63.46 (1.25)	58.80 (1.17)	54.24 (1.08)	54.54 (1.08)	58.55 (1.16)

Beijing and News; more in Appendix E. If a generator concentrates probability mass near training examples (memorization), the blue distribution exhibits a systematic left-shift toward zero relative to red, indicating that synthetic samples preferentially occupy "training neighborhoods" across distance scales. Conversely, strong overlap between the two distributions indicates that synthetic samples lie in neighborhoods that are similarly populated by unseen held-out records, suggesting little geometry-driven membership advantage over a range of neighborhood radii. We observe that for TabKDE, TabSYN, and CoreTabKDE these distributions are multi-modal, but still match almost perfectly. On the other hand SMOTE has a very different distribution, and the synthetic to train (blue) is always much smaller (typically very close to 0), indicating it may often reproduce the training data. Results for all datasets are provided in Figure 11 in the Appendix.

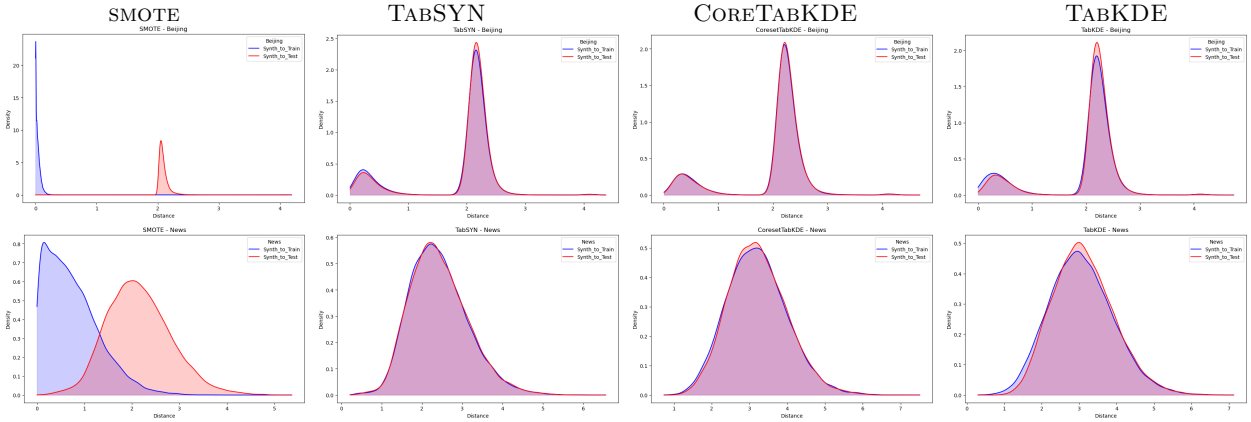

Figure 6: Privacy comparison based on DCR distributions for synthetic to training data (blue) and synthetic to held-out data (red). First row Beijing and second row News.

DCR as an implicit linkage and membership advantage. The DCR score p is the fraction of synthetic points that lie closer (under a fixed distance metric) to the training set than to the held-out set. For interpretability, we map p to odds,

$$\text{odds} = \frac{p}{100 - p},$$

which quantifies the strength of this proximity bias (e.g., $p = 58\%$ yields $1.38\times$ odds, while $p = 95\%$ yields $19\times$ odds). Viewed this way, DCR is not intended to characterize a fully informed attacker; rather, it provides a conservative, geometry-driven diagnostic of whether the released synthetic data systematically clusters around training records in a manner that could facilitate downstream linkage.

Table 11: DCR expressed as nearest-neighbor attacker odds. If the DCR score is p (in %), odds are $\frac{p}{100-p}$.

Method	Adult	Default	Shoppers	Beijing	News	Average
SMOTE(Our reproduction)	10.34×	10.71×	29.86×	∞	99.00×	22.15×
CoDi	1.00×	1.08×	1.04×	1.04×	1.03×	1.04×
TabDDPM	1.05×	1.09×	1.72×	4.03×	3.83×	1.87×
TabDiff	1.00×	1.05×	1.01×	1.02×	1.04×	1.02×
TabSYN(Our reproduction)	1.05×	1.07×	1.08×	1.14×	1.03×	1.07×
PGE-Tabsyn	1.02×	1.05×	1.08×	1.03×	1.02×	1.04×
CopulaDiff	1.01×	1.04×	1.03×	1.01×	1.13×	1.04×
RandCoreTabKDE	1.65×	1.71×	1.43×	1.74×	1.25×	1.54×
CoreTabKDE	1.11×	1.18×	1.22×	1.05×	1.08×	1.13×
TabKDE	1.65×	1.74×	1.43×	1.19×	1.20×	1.41×

Table 11 reports DCR as nearest-neighbor attacker odds, where values near 1× indicate that synthetic samples are *not* systematically closer to the training set than to a held-out set (and thus exhibit little geometric "membership advantage"). Under this lens, TabKDE and its coreset variants remain comparatively benign. In particular, CoreTabKDE attains near-unity odds across all datasets (average 1.13×), indicating only a low preference for training neighborhoods. Even the full TabKDE while higher (averages 1.41×), stay far below methods that exhibit strong training-set attraction and are orders of magnitude smaller than the extreme nearest-neighbor leakage observed for SMOTE.

Coreset methods. The coreset methods CoreTabKDE and RandCoreTabKDE work nearly as well as TabKDE in terms of accuracy, and use a fraction of the space. Surprisingly, RandCoreTabKDE often has better accuracy than CoreTabKDE and is of course faster since it does not require the optimization step. However, notably, CoreTabKDE has a much improved DCR score for privacy (of about 53%), so provides a way to address that measure within the TabKDE framework. See Appendix F for a longer discussion.

3.4 Conclusion and Limitations

We introduce a new approach for tabular data generation, built with a careful combination of only classic techniques like copula transforms and KDEs. It is the first to demonstrate high scalability, accuracy, and privacy. While its DCR privacy score is not quite as strong as other methods, this can be improved with slight accuracy trade-offs through coresets. It handles, but also requires, a mix of numerical and categorical features as is common in tabular data.

LLM Disclosure. In this paper, the use of LLMs is restricted to enhancing grammar and making partial rewording adjustments.

Reproducibility Statement. We clearly describe the full TabKDE algorithm and the other hybrid models, including encoding, copula transformation, KDE sampling, and coreset construction (Sections 2 and Appendix A). Section3 outlines the datasets used, evaluation metrics, and experimental setups, while Tables 2 and 3 include compute resources and runtime information. Additional implementation details are provided in AppendicesB–F. Together, these components enable reproduction of the key results, even independently of the code. Our code is also anonymously available here: `http://github.com/tabkde/tabkde-main`

References

Martin Arjovsky and Leon Bottou. Towards principled methods for training generative adversarial networks. In *International Conference on Learning Representations*, 2017. URL `https://openreview.net/forum?id=Hk4_qw5xe`.

Samuel A. Assefa, Danial Dervovic, Mahmoud Mahfouz, Robert E. Tillman, Prashant Reddy, and Manuela Veloso. Generating synthetic data in finance: opportunities, challenges and pitfalls. In *Proceedings*

of the First ACM International Conference on AI in Finance, ICAIF '20, New York, NY, USA, 2021. Association for Computing Machinery. ISBN 9781450375849. doi: 10.1145/3383455.3422554. URL https://doi.org/10.1145/3383455.3422554.

Randall Balestriero, Jerome Pesenti, and Yann LeCun. Learning in high dimension always amounts to extrapolation. *arXiv preprint arXiv:2110.09485*, 2021.

Vadim Borisov, Kathrin Sessler, Tobias Leemann, Martin Pawelczyk, and Gjergji Kasneci. Language models are realistic tabular data generators. In *The Eleventh International Conference on Learning Representations*, 2023. URL https://openreview.net/forum?id=cEygmQNOeI.

Nitesh V. Chawla, Kevin W. Bowyer, Lawrence O. Hall, and W. Philip Kegelmeyer. Smote: synthetic minority over-sampling technique. *J. Artif. Int. Res.*, 16(1):321–357, June 2002. ISSN 1076-9757.

Bin Dai and David Wipf. Diagnosing and enhancing VAE models. In *International Conference on Learning Representations*, 2019. URL https://openreview.net/forum?id=B1e0X3C9tQ.

Prafulla Dhariwal and Alexander Quinn Nichol. Diffusion models beat GANs on image synthesis. In A. Beygelzimer, Y. Dauphin, P. Liang, and J. Wortman Vaughan (eds.), *Advances in Neural Information Processing Systems*, 2021. URL https://openreview.net/forum?id=AAWuCvzaVt.

Joao Fonseca and Fernando Bacao. Tabular and latent space synthetic data generation: a literature review. *Journal of Big Data*, 10(1):115, 2023. doi: 10.1186/s40537-023-00792-7. URL https://doi.org/10.1186/s40537-023-00792-7.

Sébastien Gambs, Frédéric Ladouceur, Antoine Laurent, and Alexandre Roy-Gaumond. Growing synthetic data through differentially-private vine copulas. *Proceedings on Privacy Enhancing Technologies*, 2021:122 – 141, 2021. URL https://api.semanticscholar.org/CorpusID:232352028.

Mikel Hernandez, Gorka Epelde, Ane Alberdi, Rodrigo Cilla, and Debbie Rankin. Synthetic data generation for tabular health records: A systematic review. *Neurocomputing*, 493:28–45, 2022.

Jonathan Ho, Ajay Jain, and Pieter Abbeel. Denoising diffusion probabilistic models. In H. Larochelle, M. Ranzato, R. Hadsell, M.F. Balcan, and H. Lin (eds.), *Advances in Neural Information Processing Systems*, volume 33, pp. 6840–6851. Curran Associates, Inc., 2020.

Sarang Joshi, Raj Varma Kommaraji, Jeff M. Phillips, and Suresh Venkatasubramanian. Comparing distributions and shapes using the kernel distance. In *Proceedings of the Twenty-Seventh Annual Symposium on Computational Geometry*, SoCG '11, pp. 47–56, New York, NY, USA, 2011. Association for Computing Machinery. ISBN 9781450306829. doi: 10.1145/1998196.1998204. URL https://doi.org/10.1145/1998196.1998204.

Jayoung Kim, Chaejeong Lee, and Noseong Park. STasy: Score-based tabular data synthesis. In *The Eleventh International Conference on Learning Representations*, 2023. URL https://openreview.net/forum?id=1mNssCWt_v.

Akim Kotelnikov, Dmitry Baranchuk, Ivan Rubachev, and Artem Babenko. Tabddpm: modelling tabular data with diffusion models. In *Proceedings of the 40th International Conference on Machine Learning*, ICML'23. JMLR.org, 2023.

Chaejeong Lee, Jayoung Kim, and Noseong Park. Codi: co-evolving contrastive diffusion models for mixed-type tabular synthesis. In *Proceedings of the 40th International Conference on Machine Learning*, ICML'23. JMLR.org, 2023.

Tennison Liu, Zhaozhi Qian, Jeroen Berrevoets, and Mihaela van der Schaar. GOGGLE: Generative modelling for tabular data by learning relational structure. In *The Eleventh International Conference on Learning Representations*, 2023. URL https://openreview.net/forum?id=fPVRcJqspu.

Yanchen Luo, Junfeng Fang, Sihang Li, Zhiyuan Liu, Jiancan Wu, An Zhang, Wenjie Du, and Xiang Wang. Text-guided small molecule generation via diffusion model. *iScience*, 27(11):110992, 2024.

Aref Majdara and Saeid Nooshabadi. Nonparametric density estimation using copula transform, bayesian sequential partitioning, and diffusion-based kernel estimator. *IEEE Transactions on Knowledge and Data Engineering*, 32(4):821–826, 2020. doi: 10.1109/TKDE.2019.2930052.

Josep Maria Mateo-Sanz, Francesc Sebé, and Josep Domingo-Ferrer. Outlier protection in continuous microdata masking. In Josep Domingo-Ferrer and Vicenç Torra (eds.), *Privacy in Statistical Databases*, pp. 201–215, Berlin, Heidelberg, 2004. Springer Berlin Heidelberg. ISBN 978-3-540-25955-8.

D. Meyer, T. Nagler, and R. J. Hogan. Copula-based synthetic data augmentation for machine-learning emulators. *Geoscientific Model Development*, 14(8):5205–5215, 2021. doi: 10.5194/gmd-14-5205-2021. URL https://gmd.copernicus.org/articles/14/5205/2021/.

Alex Morehead and Jianlin Cheng. Geometry-complete diffusion for 3d molecule generation and optimization. *Communications Chemistry*, 7(1):150, 2024.

Yidong Ouyang, Liyan Xie, Chongxuan Li, and Guang Cheng. Missdiff: Training diffusion models on tabular data with missing values. In *ICML 2023 Workshop on Structured Probabilistic Inference & Generative Modeling*, 2023. URL https://openreview.net/forum?id=S435pkeAdT.

Neha Patki, Roy Wedge, and Kalyan Veeramachaneni. The synthetic data vault. In *2016 IEEE International Conference on Data Science and Advanced Analytics (DSAA)*, pp. 399–410, 2016. doi: 10.1109/DSAA.2016.49.

Jeff M. Phillips. Coresets and sketches. In *Handbook of Discrete and Computational Geometry*, chapter 49. CRC Press, 2016.

Jeff M. Phillips and Wai Ming Tai. Near-optimal coresets of kernel density estimates. *Discrete & Computational Geometry*, 63(4):867–887, 2020. doi: 10.1007/s00454-019-00134-6. URL https://doi.org/10.1007/s00454-019-00134-6.

Robin Rombach, Andreas Blattmann, Dominik Lorenz, Patrick Esser, and Bjorn Ommer. High-Resolution Image Synthesis with Latent Diffusion Models . In *2022 IEEE/CVF Conference on Computer Vision and Pattern Recognition (CVPR)*, pp. 10674–10685, Los Alamitos, CA, USA, June 2022. IEEE Computer Society. doi: 10.1109/CVPR52688.2022.01042. URL https://doi.ieeecomputersociety.org/10.1109/CVPR52688.2022.01042.

Nasir Saukani and Noor Azina Ismail. Identifying the components of social capital by categorical principal component analysis (catpca). *Social Indicators Research*, 141(2):631–655, 2019.

D. W. Scott. *Multivariate Density Estimation: Theory, Practice, and Visualization*. 2015.

Juntong Shi, Minkai Xu, Harper Hua, Hengrui Zhang, Stefano Ermon, and Jure Leskovec. Tabdiff: a mixed-type diffusion model for tabular data generation. In *The Thirteenth International Conference on Learning Representations*, 2025. URL https://openreview.net/forum?id=swvURjrt8z.

B. W. Silverman. *Density Estimation for Statistics and Data Analysis*. Chapman & Hall, London, 1986.

Amy Steier, Lipika Ramaswamy, Andre Manoel, and Alexa Haushalter. Synthetic data privacy metrics, 2025. URL https://arxiv.org/abs/2501.03941.

Lei Xu, Maria Skoularidou, Alfredo Cuesta-Infante, and Kalyan Veeramachaneni. *Modeling tabular data using conditional GAN*. Curran Associates Inc., Red Hook, NY, USA, 2019.

Hengrui Zhang, Jiani Zhang, Zhengyuan Shen, Balasubramaniam Srinivasan, Xiao Qin, Christos Faloutsos, Huzefa Rangwala, and George Karypis. Mixed-type tabular data synthesis with score-based diffusion in latent space. In *The Twelfth International Conference on Learning Representations*, 2024. URL https://openreview.net/forum?id=4Ay23yeuz0.

A TabKDE Algorithm

The TabKDE algorithm is a simple, scalable, and privacy-aware method for generating high-fidelity synthetic tabular data. It implements the general framework (see Section 1) for tabular generation; the key innovation is in the mapping to latent space and generative modeling sets. These steps are simple and efficient while satisfying our desiderata. We overview them here:

TabKDE Latent Space Mapping: This is accomplished in two parts. The first step is a copula-based transformation of the tabular dataset $\mathcal{T}$ into a latent representation Z that lies within the continuous space $[0,1]^d$, allowing precise control over the domain of the marginal distributions. Second is estimating the covariance Σ of data in this space, implicitly defining a Mahalanobis distance which captures the similarity within this latent domain.

TabKDE Generative Modeling: Here we use a KDE model to allow for a non-parametric complex distributional model. We simply sample by choosing a training data point in the latent space $z \sim \mathsf{Unif}(Z)$, and then chose a random direction u scaled by the covariance Σ. Then we generate a new point

$$z' \leftarrow z + ur$$

where r is a scalar amount controlling the amount of deviation from the training data. In particular, we select r at random from a learned distribution from the training data estimating the distance to the closest point. One more idea is needed, we want to disallow points outside $[0,1]^d$ to respect the original column marginals. To handle this, we keep coordinates in $[0,1]^d$, and regenerate the others iteratively.

We next describe all aspects in more detail.

A.1 Encoding of Tabular Features: $\mathcal{T} \to E$

Let $\mathcal{T} = \{X_1, \ldots, X_n\}$ be a real data set. Before transforming tabular data into a latent space, it is essential to convert all feature types into a unified numerical format $\mathcal{T} \mapsto E \in \mathbb{R}^{n \times d}$, suitable for further processing. Note that the new representation E has n rows (one for each row of the table $\mathcal{T}$), and more importantly d columns (one for each column of the table $\mathcal{T}$). This means, do not use one-hot-encoding, and this will be essential for our representation and sampling from the latent space to ensure marginal properties of each data column.

In this section, we describe how we handle numerical, ordinal, and categorical features through encoding strategies designed to preserve basic structural relationships and facilitate meaningful downstream transformations.

Numerical and Ordinal Mapping. All numerical columns are z-score normalized (parameters fit on the training data, saved, and used to de-normalize synthetic outputs back to the original units), so values are reported on the original scale. Ordinal features are simply converted to consecutive integers $1, 2, \ldots,$ that preserve their inherent order. This ensures that the ordinal relationships between categories are preserved while converting them into numerical representations.

Categorical Mapping. For categorical features, we use a data-driven approach to map each unique category to a continuous space based on the statistical properties of the numerical features in the data.

Recall that $\mathsf{Cat} = \{d_2 + 1, \ldots, d\}$ denotes the set of indices corresponding to categorical features. Additionally, assume that for each $j \in \mathsf{Cat}$, the number of unique categories in the j-th feature is given by $|C_j| = k_j$. Define $Z \in \mathbb{R}^{n \times d_1}$ as the matrix obtained by selecting only the numerical features from the dataset, and let u represent its first principal component scores (PC1 scores) obtained using Principal Component Analysis (PCA) ($u = Zv$ where v is top principal vector of Z). Let $j \in \mathsf{Cat}$ be an arbitrary categorical feature with unique category set $C_j = \{c_1, \ldots, c_{k_j}\}$. For each category $c \in C_j$, we identify the corresponding row indices in D, defined as

$$I_{j,c} = \{i \in [n] \mid (X_i)_j = c\}.$$

We then assign each category c the value

$$v_{j,c} = \frac{1}{|I_{j,c}|} \sum_{i \in I_{j,c}} u_i,$$

This value represents the average of the first principal component scores u_i for all instances where the j-th categorical feature takes the value c. This process is summarized in the following algorithm.

Algorithm 5 PRINCIPALGUIDEDENCODING($\mathcal{T}$, Cat, Num)

1: Compute u as the first principal component scores of X_{Num}; which contains only numerical features in $\mathcal{T}$.
2: **for** each category $c \in C_j$, in each categorical feature $j \in$ Cat:

$$v_{j,c} \leftarrow \frac{1}{|I_{j,c}|} \sum_{i \in I_{j,c}} u_i, \quad \text{where } I_c = \{i \in [n] \mid (X_i)_j = c\}$$

3: **for** each data $(X_i)_j = c \in C_j$, for each categorical feature $j \in$ Cat: $(E_i)_j \leftarrow v_{j,c}$

PGE can be interpreted as using the leading principal component scores of the numerical block as a one-dimensional "ruler": each category is embedded as a scalar given by the mean PCA score of the rows in which it appears. When categorical semantics are mediated through numerical covariates, this construction tends to place categories with similar co-occurring numerical profiles nearby along that dominant direction, yielding a continuous embedding that preserves meaningful neighborhood relations. Because the code for each category is learned from the numerical block, PGE helps retain *cat–num* dependence and can also reflect *cat–cat* structure that is induced via shared numerical correlates. In contrast, column-wise encodings such as uniform or frequency mappings depend only on the marginal distribution of the categorical column, and thus cannot incorporate cross-type associations by construction. See Section 3.2 for some related ablation study.

A.2 Map to Numerical Latent Space: $E \to Z$

Notably, after the initial encoding step (Subsection A.1), all features in the dataset are converted into numerical values, resulting in a representation that lies in a subset of $\mathbb{R}^d$. Our goal is to further transform this representation into a continuous latent space within the unit hypercube $[0,1]^d$, where the dependencies between features are preserved, and the data is appropriately normalized to ensure that all numerical features contribute equally, making it well-suited for downstream tasks such as sampling and density estimation.

The algorithm outlined below–MAPTOLATENTSPACE–provides a high-level overview of this transformation process. It combines ordinal encoding, a structure-aware encoding of categorical features, and a copula-based normalization of all features. While this procedure is presented here in full, each of its core components will be introduced and discussed in detail in the subsequent sections.

Algorithm 6 MAPTOLATENTSPACE($\mathcal{T}$, Num, Cat, Ord)

1: Mapped each ordinal feature to integers reflecting its natural order.
2: Encoded categorical features by PRINCIPALGUIDEDENCODING($\mathcal{T}$, Cat, Num)
3: Concatenate numerical and the transformed ordinal and encoded categorical features to obtain E
4: Convert the encoded data E into $Z = \text{COPULAMAPPING}(E) \in [0,1]^{n \times d}$.
5: **return** Z

Before exploring the details of this mapping, we first introduce foundational concepts from the copula method—a well-established statistical technique that separates marginal distributions from the dependency structure in multivariate data.

Introduction to Copula Transformation. In many real-world datasets, variables exhibit complex dependencies, making it challenging to model their joint distribution directly. Copula method provides a

powerful statistical tool to decouple the dependency structure from the marginal distributions, allowing for more flexible data transformations. The copula method invertibly transforms a dataset $E \in \mathbb{R}^{n \times d}$, consisting of d-dimensional features, into a new representation $Z \in [0,1]^{n \times d}$ and as a result, each individual record in Z lies in $[0,1]^d$, and the marginal distributions of Z are uniform over the interval $[0,1]$. We next examine the underlying mechanism by which this transformation is achieved.

1. **Copula Forward Transformation (Mapping E to Z)**: For each dimension j (where $j = 1, \ldots, d$), we compute the empirical cumulative distribution function (ECDF) of the j-th feature:

$$\begin{aligned} \hat{F}_j(x) &= \Pr(\text{value of } j\text{-th coordinate} \leq x) \\ &= \frac{1}{n} \sum_{i=1}^{n} \mathbb{I}(x_{ij} \leq x) \end{aligned}$$

where $\mathbb{I}(x_{ij} \leq x)$ is an indicator function that equals 1 if $x_{ij} \leq x$, and 0 otherwise. In summary, $\hat{F}_j(x)$ represents the proportion of observations in the dataset whose j-th coordinates are less than or equal to x. Each coordinate value x_{ij} is then transformed into a uniform representation:

$$z_{ij} = \hat{F}_j(x_{ij}) \tag{1}$$

This ensures that each feature is uniformly mapped into the interval $[0,1]$, producing a dataset Z that follows a uniform distribution for each of its marginals while maintaining the dependency structure of X.

Algorithm 7 CopulaMapping(E)

1: For each feature j, compute empirical CDF value $\hat{F}_j(x_{i,j})$ for $D_j = \{x_{1j}, \ldots, x_{nj}\}$.
2: Set $z_i = (z_{i,1}, \ldots, z_{i,d})$, where $z_{i,j} = \hat{F}_j(x_{i,j})$
3: **return** $Z = \{z_1, \ldots, z_n\}$

Using the Copula transformation, we effectively *standardize* the data set into a unit hypercube, making it more suitable for density estimation, sampling, and synthetic data generation. Furthermore, this method allows for *dependency-preserving transformations*, ensuring that the statistical relationships between variables are retained even when synthetic data is produced.

2. **Copula Inverse Transformation (Mapping Z back to E)**: It is key that we store the ECDF $\hat{F}$, because we need to be able to invert it. Its inverse cumulative distribution function (quantile function) $\hat{F}^{-1}$ is defined as

$$\hat{F}^{-1}(q) = \inf\{x \mid \hat{F}(x) \geq q\} \qquad \text{for any value} \qquad q \in [0,1].$$

Given $z = (z_1, \ldots, z_d) \in [0,1]^d$, each feature j can be mapped back to its initial numerical representation using the inverse cumulative distribution function $\hat{F}_j^{-1}(\cdot)$.

Decoding. We can also decode the output E to the structure in the table. For an ordinal or categorical feature j, we apply probabilistic rounding to the two nearest categories (in the initial numerical embedding), with the probabilities proportional to their distance to p_j. Also, for numerical features, the value is reconstructed (up to the appropriate precision) by interpolating between the two closest values (in the original distribution) to p_j, with the interpolation weights determined by their distance from p_j. This step ensures that the generated samples maintain the same marginal distributions as the original dataset.

Algorithm 8 InverseECDF($z = (p_1, \ldots, p_d), \{\hat{F}_i : i \in [d]\}$)

for each $j \in [d]$:
  if $\min(\{z_{ij}\}_{i=1}^n) \geq p_j$ or $\max(\{z_{ij}\}_{i=1}^n) \leq p_j$ **then**
    Return $\min(\{x_{ij}\}_{i=1}^n)$ or $\max(\{x_{ij}\}_{i=1}^n)$ respectively
  Let $z_{i_1} < z_{i_2}$ be consecutively ordered points so that $p \in [z_{i_1}, z_{i_2}]$
  if $j \in$ Ord or $j \in$ Cat, **then**
    Return $x_j = x_{i_1}$ with probability $\frac{|p_j - z_{i_1}|}{|z_{i_1} - z_{i_2}|}$ and otherwise x_{i_2}.
  elseif $j \in$ Num, **then**
    Return

$$x = x_{i_2} + \frac{|p_j - z_{i_2}|}{|z_{i_1} - z_{i_2}|}(x_{i_1} - x_{i_2}) \tag{2}$$

A.3 Sensitivity Analysis of the Encoding–Decoding Pipeline

PGE represents each category c by scalar $v_{j,c}$: the mean of first principal component scores u (PC1 scores) restricting to value c in column j. It is computed from the z-score normalized numerical block, making it insensitive to affine rescaling of the raw numerical columns. TabKDE then applies a per-coordinate empirical-copula transform (ECDF), which depends only on ranks of these scalars and therefore further reduces sensitivity to monotone re-parameterizations of each coordinate. Note that statistically this is almost impossible to different categories $c \neq c'$ receive same value $v_{j,c} = v_{j,c'}$. During decoding, categorical and ordinal coordinates are recovered via probabilistic rounding to the two nearest embedded codes using the inverse ECDF (which is computed on ranks), so categories become indistinguishable only in the presence of exact ties in their learned codes. Finally, as shown in Section 3.2, TabKDE is robust to replacing PGE with alternative single-scalar encodings like frequency or uniform.

A.4 Learning Distance to Closest Record (DCR)

A central use of synthetic data is as a proxy for private personal data. So it is paramount to ensure that the synthetic data process is not leaking too much information about the original data. A common measurement of this is **Distance to Closest Record (DCR)** (Mateo-Sanz et al., 2004; Steier et al., 2025) which evaluates how similar a synthetic record x_s is to a real one from a set D. It is formally defined for an appropriate distance metric $\mathtt{d}$ as:

$$\mathrm{DCR}(x_s, D) = \min_{x_r \in D} \mathtt{d}(x_s, x_r) \tag{3}$$

A DCR of 0 indicates an identical match, posing a significant privacy risk. Comparing DCR values between synthetic data and both training D_T and holdout D_H datasets helps assess privacy. If synthetic records are much closer to the training data, it suggests the model may be memorizing real data. Ideally, for synthetic data S, DCR distributions $\{\mathrm{DCR}(x_s, D_T)\}_{x_s \in S}$ and $\{\mathrm{DCR}(x_s, D_H)\}_{x_s \in S}$ **should heavily overlap**, showing that synthetic data reflects general patterns rather than replicating specific records.

As part of our generative process, we learn this distribution in the copula latent embedding Z using *Euclidean distance*. Then we can generate synthetic data to mirror this scale of variation. We repeatedly randomly split the training data Z, and compute the DCR distribution between the two splits (see EmpiricalDCR; Alg. 9). Then it fits a simple mixture of Gaussians model to this distribution; using Bayesian Information Criterion (BIC)[3], we select the best model for $k = 1, \ldots, 10$ as the number of components.

[3] `https://scikit-learn.org/stable/modules/generated/sklearn.mixture.GaussianMixture.html#sklearn.mixture.GaussianMixture.bic`

Algorithm 9 EMPIRICALDCR(Z): Estimating the Empirical DCR Distribution

```
Initialize L = []
for i = 1, ..., T do
    Partition Z into two random equal-sized subsets Z_1 and Z_2.
    for each z_2 ∈ Z_2 do
        Compute the minimum distance between z_2 and the records in Z_1.
        Add this distance to L.
Fit a mixture of k Gaussian components to L.
```

A.5 Tabular Kernel Density Estimation: $Z \to$ Sample

KDE (Kernel Density Estimation) is a non-parametric method used to estimate the probability density function (PDF) of a continuous random variable by smoothing finite data points with a kernel function (typically Gaussian). Its accuracy depends on bandwidth selection and data availability (Silverman, 1986; Scott, 2015). It can also be used to generate synthetic data by fitting a KDE model to the existing dataset and drawing samples from it. We now formally define KDE.

Assuming that $X = \{x_1, x_2, \ldots, x_n\}$ is a dataset in $\mathbb{R}^d$, the Kernel Density Estimation (KDE) is given by:

$$\hat{f}(x) \propto \frac{1}{n} \sum_{i=1}^{n} K\left(\frac{x - x_i}{h}\right)$$

where:

- $\hat{f}(x)$ is the estimated likelihood at point x,
- $K(\cdot)$ is a centrally-symmetric kernel function (e.g., Gaussian kernel),
- $h > 0$ is the bandwidth parameter controlling smoothness.

Sampling from KDE. To sample from a KDE_X, we simply sample a point $x \in X$, and then sample a point nearby proportional to the kernel likelihood. For example, with a isotropic Gaussian kernel, using this approach, a synthetic data point is generated as $x \sim \mathcal{N}(x_i, \frac{h}{2}I);\ x_i \sim X$. However, we do not use a Gaussian kernel, as this is not adaptive to the DCR distribution – which may be multi-modal. So we use our EMPIRICALDCR(Z) estimate to define our kernel. Still, this approach may raise a couple of concerns:

- At first glance, one may worry that this approach does not guarantee preservation of DCR, since it might use our kernel $K(x_i, \cdot)$ to generate a point nearby x_i that lands too close to another $x' \in X$. However, this is not observed to be an issue, as generation in high-dimensional space makes it highly unlikely to produce points close to other points in the training data (see Subsection 2.3).
- Second, the sampled point x may fall outside the convex hull of the dataset X, potentially resulting in unrealistic data generation. We address this by using the sample covariance Σ to guide the perturbation direction. And moreover, some form of extrapolation in this sense is probably necessary and unavoidable (Balestriero et al., 2021), and we believe desirable. Yet, violating the marginals associated with individual table columns, we find, can distort distributions (see Subsection G.1). This issue is addressed by generalizing SIMPLEKDE to a more advanced method, TABKDE, which controls for this.

To resolve the first issue, we estimate the DCR distribution using Algorithm 9 (EMPIRICALDCR) and leverage it to strategically perturb the sampled point x_i. We summarize this approach by the following algorithms: Algorithm 10 SIMPLEKDE($\mathcal{T}$), which iteratively calls Algorithm 11 SAMPLEKDE(Z, f, Σ) using the copula-transformed data Z, its estimated DCR distribution f, and its estimated covariance Σ.

Algorithm 10 SimpleKDE($\mathcal{T}$)

1: Transform table $\mathcal{T}$ into $Z \in [0,1]^{n \times d}$ as $Z \leftarrow$ CopulaTransform($\mathcal{T}$, Num, Cat, Ord)
2: $\Sigma \leftarrow$ Covariance(Z)
3: Estimate empirical DCR distribution $f =$ EmpiricalDCR(Z)
4: **for** $i = 1, \ldots, m$:
5: $\quad z'_i =$ SampleKDE(Z, f, Σ)
6: $\quad y_j \leftarrow$ InverseECDF(z'_j, j-th feature type, F_j)
7: **return** $Y = \{y_1, \ldots, y_m\}$

Algorithm 11 SampleKDE(Z, f, Σ)

1: Uniformly sample $z_i \in Z$
2: Sample radius $r > 0$ from f
3: Sample $v \sim \mathcal{N}(0, \Sigma)$, set $u = \frac{v}{\|v\|}$
4: **return** $z' \leftarrow z_i + r \cdot u$

As discussed in Subsection G.1, the SimpleKDE algorithm does not explicitly control the support of the marginals and, in particular, does not fully address the second challenge outlined earlier. The copula-transformed representation, however, embeds the data within the unit hypercube, which allows us to control how far a perturbed sampled point x can deviate without violating marginal support. We now introduce a more refined rejection-sampling heuristic (Alg. 12: TabKDE) that effectively enforces these boundary constraints.

Algorithm 12 TabKDE(X)

1: Transform table $\mathcal{T}$ into $Z \in [0,1]^{n \times d}$ as $Z \leftarrow$ CopulaTransform($\mathcal{T}$, Num, Cat, Ord)
2: $\Sigma \leftarrow$ Covariance(Z)
3: Estimate empirical DCR distribution $f =$ EmpiricalDCR(Z)
4: **for** $i = 1, \ldots, m$:
5: $\quad z'_i =$ SampleKDE-iterative(Z, f, Σ)
6: $\quad y_i =$ InverseCopula(z'_i)
7: **return** $Y = \{y_1, \ldots, y_m\}$

TabKDE differs from SimpleKDE only in the sampling step at line 5, where it uses the boundary-aware SampleKDE-iterative instead of the simpler SampleKDE. This modified sampler actively checks for violations of the unit hypercube boundaries and iteratively adjusts any out-of-bound coordinates. If a valid point cannot be obtained after a fixed number of attempts, the sample is discarded, and the process restarts. This mechanism guarantees that all accepted samples lie within the latent space $[0,1]^d$.

Algorithm 13 SampleKDE-iterative(Z)

Uniformly sample $z_i \in Z$
Sample radius $r > 0$ from f
Sample $v \sim \mathcal{N}(0, \Sigma)$, set $u = \frac{v}{\|v\|}$
$z' \leftarrow z_i + r \cdot u$
While $\{j : z'_j \notin [0,1]\} \neq \varnothing$:
    $J \leftarrow \{j : z'_j \notin [0,1]\}$
    Sample $v' \sim \mathcal{N}(0, \Sigma)$, set $w = \frac{v'}{\|v'\|}$
    $s \leftarrow \frac{\|(u_k)_{k \in J}\|}{\|(w_k)_{k \in J}\|}$
    $u_j \leftarrow s \cdot w_j$ for each $j \in J$
    $z' \leftarrow z_i + r \cdot u$
return z'

B Experimental Setup and Data

B.1 Datasets

Our experiments are conducted on the six tabular datasets from UCI Machine Learning Repository[4] (Adult, Default, Shoppers, Magic, Beijing, News) used in TabSYN (Zhang et al., 2024), along with the IBM dataset[5] which is significantly larger. In all they covering a wide range of domains for tabular data. These datasets include a mix of numerical and categorical features and vary in the number of points, feature types, and task types (classification or regression), making them well-suited for evaluating the generalizability of synthetic data generation methods. A few of the categorical features can be interpreted as ordinal; but outside the IBM dataset, we simply treat them as categorical. We summarize their traits in Table 12.

Table 12: Dataset statistics. **Num** denotes the number of numerical columns, **Cat** the number of categorical columns, **Ord** the number of ordinal features, and **Sum Cat** the total number of unique categories across all categorical and ordinal columns. Ordinal features can be treated as categorical features by disregarding their inherent order; note $(*)$ that we do this for the Adult and Default datasets. For the IBM dataset, we randomly select two 200k subsamples to serve as the training and testing sets; we ensured that the test set contains no categorical values unseen in the training set. In IBM data, we treat "*Year*", "*Month*", "*Day*", "*Time*", "*Zip*" features as ordinal. (†) In TabKDE, simple-KDE, CopulaDiff and CoreTabKDE, for Beijing dataset, we treat the features "Is", "Ir", and "Iws" as categorical, and for the Shoppers dataset, we apply the same treatment to the features "SpecialDay", "ProductRelated", and "Informational". For all of these features, the ratio of unique values in the training set to the total number of data points is very low, with the majority of occurrences concentrated on a single value.

Dataset	Total	Train	Test	Num	Cat	Ord	Sum Cat	Task
Adult	48,842	32,561	16,281	6	7	2*	120	Classification
Default	30,000	27,000	3,000	14	9	1*	79	Classification
Shoppers†	12,330	11,097	1,233	10	8	0	67	Classification
Magic	19,019	17,117	1,902	10	1	0	2	Classification
Beijing†	41,757	37,581	4,176	7	5	0	76	Regression
News	39,644	35,679	3,965	46	2	0	13	Regression
IBM	341,675	176,221	165,454	1	8	5	37,721	Classification

Split of the Data. We consider two ways to split data into test and train set. The numbers in Table 12 reflects the splits done by TabSYN, which we maintain for direct comparison. This split was not even in size, partially to ensure there were no categories in the Test split which were not present in the Train split. When we do not directly compare to results in the (Zhang et al., 2024), we use a different random and even split.

[4] `https://archive.ics.uci.edu/datasets`
[5] https://www.kaggle.com/code/yichenzhang1226/ibm-credit-card-fraud-detection-eda-random-forest

Again, following the TabSYN paper (Zhang et al., 2024), the target column is treated as either numerical or categorical based on the task type: it is considered categorical for classification tasks and numerical otherwise. For the Machine Learning Efficiency experiments, each dataset is divided into training, validation, and testing sets. For the Adult dataset, we use its official testing set, while the original training set is further split into training and validation sets with an 8:1 ratio. All other datasets are split into training, validation, and testing sets using an 8:1:1 ratio with a fixed random seed.

To get the IBM dataset to run, we needed to leverage the ordinal representation in variables Year, Month, Day, Time, and Zip. We also identify that the Merchant State and Merchant City are very strongly correlated with Zip (the zip code), and since these categories are often quite rare, we applied another modeling (called *reduced modeling*) to improve the generation. We put Zip in the generative model, but not Merchant City or Merchant State. Then once we generate a Zip, we predict the the Merchant City and Merchant State. We use the same process with the correlated MCC and Merchant Name; we put MCC in the generative model, and use the outcome to predict Merchant Name. For transparency, we however report results both with and without this reduced modeling trick (see Table 21 and Figure 10).

B.2 Baselines

We compare our proposed TabKDE method with several popular baselines, including SMOTE (Chawla et al., 2002), CTGAN(Xu et al., 2019), TVAE (Xu et al., 2019), GReaT (Borisov et al., 2023), GOGGLE (Liu et al., 2023), CoDi (Lee et al., 2023), STaSy (Kim et al., 2023), TabDDPM (Kotelnikov et al., 2023), TabSYN (Zhang et al., 2024), and TabDiff (Shi et al., 2025)[6]. Through this comparison, we demonstrate that TabKDE provides a simpler, faster, and more scalable alternative for generating realistic synthetic tabular data, without significantly compromising on quality or privacy.

By abstracting to the general framework (outlined in Section 1) we are able to also consider several hybrid models that mix elements of TabKDE with the encoding choices, the VAE method, or the diffusion-driven generation made popular through TabSYN and others. We specifically consider

- **CopulaDiff:** We first use our CopulaMapping (Alg. 7) to embed data into a latent space, train a Diffusion model there, and then map the generated samples back to the original space.
- **VAETabKDE:** This model trains a VAE to embed data into numerical space (as in TabSYN), then applies the Copula and KDE methods to generate samples, which are then mapped back to the original tabular format.
- **VAESimpleKDE:** VAESimpleKDE differs from VAETabKDE only in the sampling step, analogous to how TabKDE differs from simple-KDE.
- **PGE-Tabsyn:** In the method we replace one-hot encoding with the encoding outlined in Subsection A.1 (see the first three steps in MapToLatentSpace Alg. 6), which tokenizes the tabular data into the space E before applying VAE and Diffusion models.

B.3 Evaluation

To evaluate our synthetic data generation method, we focus on three main objectives including **1) Scalability**, **2) Accuracy**, and **3) Privacy**. In terms of Efficiency, we measure and compare the training and sampling time required by each model across various datasets. For Accuracy, we assess how well the synthetic data captures (1) the ground truth marginals for each column individually, (2) correlations for pairs of columns, (3) the entire distribution using machine learning efficiency, and (4) the balance between fidelity and coverage using α-Precision and β-Recall. For Privacy, we use the Distance to Closest Records (DCR) metric to assess privacy protection by measuring how similar the synthetic data is to the training/test data sets.

[6]We have not yet been able to reproduce all results for TabDiff, but they report (Shi et al., 2025) very similar performance to TabSYN in terms of accuracy, efficiency, and privacy – although with small, but noticeable improvement on categorical data. This follows since they build directly on most of the framework of TabSYN except for using a discrete diffusion on the categorical parts. For the comparison to TabKDE and its relatives, TabSYN's performance should serve as a good empirical representative.

C Scalability and Efficiency

We measure the scalability and efficiency on both the training time, as well as the sample generation time; this second part is the generation of a sample the same size as the training set. As shown in Tables 13 and 14, we see in most existing methods the time is almost entirely dominated by the training aspect. However, TabKDE the training and sampling are more comparable because the training time is so much lower.

All our experiments, unless otherwise specified, were conducted using only the CPU of a 2021 Apple MacBook Pro (14-inch), equipped with an Apple M1 Pro chip. This device features an 8-core CPU (comprising 6 performance cores and 2 efficiency cores) and 16 GB of unified memory. Table 13 presents a comparison of the training times between TabSYN and SMOTE against our proposed TabKDE, demonstrating that our method is highly computationally efficient and can be effectively executed on a standard consumer-grade laptop. TabSYN and SMOTE both run out of memory on the IBM data set, this is primarily because it has a huge number of categories, and these methods rely on one-hot encoding, which blows up the dimensionality into a 37,733-dimensional space. The memory inefficient one-hot encoding is standard in many modern models. SMOTE requires this dimensionality to identify the k nearest neighbors, which becomes highly inefficient in such a high-dimensional space (see Table 12 for dataset details).

In contrast, our proposed tokenization method, PrincipalGuidedEncoding (Algorithm 5), transforms tabular data into a numerical format with a fixed dimensionality equal to the original number of features (14 in this case, compared to 37722 with one-hot encoding), providing a far more efficient representation.

Table 13: Runtime comparison of Tabsyn, TabKDE, and SMOTE models across individual datasets on laptop. The IBM dataset is excluded from the average row.

Dataset	TabSYN				SMOTE	TabKDE	
	VAE Train	Diff. Train	Total Train	Sample	Train+Sample	Train	Sample
Adult	6h 35m 43s	2h 6m 31s	8h 43m 19s	1m 5s	4s	44s	20s
Default	6h 32m 3s	2h 2m 16s	8h 34m 59s	40s	2s	59s	17s
Shoppers	3h 57m 42s	0h 55m 32s	4h 53m 32s	18s	3s	17s	5s
Magic	3h 51m 7s	1h 21m 27s	5h 13m 0s	26s	5s	19s	7s
Beijing	5h 31m 57s	1h 57m 44s	7h 30m 35s	54s	2s	35s	16s
News	14h 34m 15s	2h 8m 59s	16h 44m 11s	57s	4s	6m 2s	54s
Average	**6h 50m 27s**	**1h 45m 24s**	**8h 36m 36s**	**43s**	**3s**	**1m 29s**	**19s**
IBM	OOM	OOM	OOM	OOM	OOM	10m 21s	6m 4s

The baseline methods in the TabSYN (Zhang et al., 2024) paper were evaluated on the `Adult` dataset using an NVIDIA RTX 4090 GPU with 24 GB of memory, as shown in Table 14. In contrast, our experiments—including those for TabSYN and the proposed TabKDE—were conducted entirely on significantly less powerful hardware. Despite this substantial difference in computational resources, TabKDE demonstrates superior efficiency. As shown in Table 13, it achieves an average training time of only 1 minute and 29 seconds, and a sampling time of just 19 seconds across six benchmark datasets. This is considerably faster than the TabSYN model, which requires more than 8.5 hours of training on average. These results highlight that TabKDE not only nearly matches the performance of more complex models (see Section D) but also does so at a fraction of the computational cost, making it highly suitable for deployment on standard consumer-grade machines without the need for specialized accelerators.

As previously noted, running TabSYN on the IBM dataset is infeasible given our standard computational resources. This limitation arises mainly due to using one-hot encoding—results in a 37,733-dimensional feature space. However, we can alternatively use encoding scheme introduced in the preprocessing steps of TabKDE. Accordingly, we apply both CopulaDiff and PGE-Tabsyn to the IBM dataset. Training CopulaDiff requires 15 hours and 7 minutes, while PGE-Tabsyn demands over 40 hours in total—25 hours and 56 minutes for the VAE and 14 hours and 39 minutes for the diffusion stage. As shown in Table

Table 14: Training and sampling times for baseline methods on the Adult dataset, evaluated using an NVIDIA RTX 4090 GPU with 24 GB of memory (adapted from the TabSYN (Zhang et al., 2024) paper).

Method	Training Time	Sampling Time
CTGAN	17 min 10 s	0.86 s
TVAE	5 min 53 s	0.51 s
GOGGLE	1 h 34 min	5.34 s
GReaT	2 h 27 min	2 min 19 s
STaSy	38 min 3 s	8.94 s
CoDi	2 h 56 min	4.62 s
TabDDPM	17 min 11 s	28.92 s
TabSYN	40 min 22 s	1.78 s

13, TabKDE only takes about 10 minutes of training time. This comparison further highlights TabKDE 's advantage in scalability over more resource-intensive methods.

For a direct comparison, we evaluate TabKDE alongside the baselines TabSYN, TabDDPM, CoDi, and GReat on the Adult, Default, Shoppers, and Magic datasets, using an NVIDIA RTX A5000 GPU with 24GB of memory and a maximum power draw of 230W, under the same experimental settings as TabSYN. See Tables 15 and 16 and Figure 7 for details. TabKDE is orders of magnitude faster in training, but on par with others in sampling time – we generate samples sequentially, and did not optimize for the GPU.

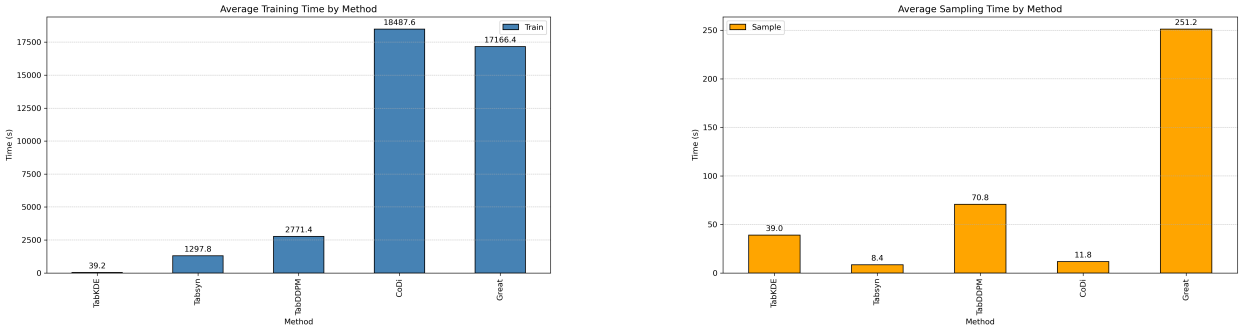

(a) Training time

(b) Sampling time

Figure 7: Average training and sampling time over Adult, Default, Shoppers, and Magic for different methods.

Table 15: Average training and sampling time for each method.

Method	Train Time (s)	Sample Time (s)
Great	17112.4	251.2
Codi	18487.6	11.8
TabDDPM	2771.4	70.8
TabSYN	1297.8	8.4
TabKDE	39.2	39.0

D Accuracy Evaluation

In this section, we evaluate the quality of the generated synthetic data using three criteria: (1) marginal distribution alignment, (2) pairwise correlation matching, and (3) finally global alignment between synthetic and hold-out distributions is compared by how well a classifier can separate the distributions.

Table 16: Average training and sampling times (in seconds)± standard deviation for each dataset using the TabKDE model. Values are reported as mean and standard deviation over 10 repeated runs.

Dataset	Train Time (s)	Sample Time (s)
Adult	51.50±1.08	50.30±0.67
Default	45.00±0.67	55.10±0.99
Shoppers	21.50±0.53	18.20±0.42
Magic	33.00±0.67	21.00±0.67
Beijing	63.00±0.47	51.80±0.79
News	64.30±1.16	166.80±1.32
Average	**46.38**±0.29	**60.53**±0.42

D.1 Marginal distribution alignment

When evaluating synthetic tabular data, **marginal distribution alignment score** assesses how closely each individual column matches its real-data distribution represented by train data. Following what was done in the TabSYN paper, we calculate the Kolmogorov–Smirnov (KS) distance for numerical attributes in Num and the Total Variation Distance for categorical and ordinal attributes in Cat and Ord. Table 17 presents, for each dataset, the average marginal alignment errors across all features for each method. Table 18 presents the performance of the TabKDE model in aligning marginal distributions, averaged over 10 runs.

Table 17: Performance comparison on marginal distribution alignment (Error rate %). Lower values indicate better performance. The values in parentheses denote the ratio relative to the smallest value. Baseline values, unless stated otherwise, are taken from (Zhang et al., 2024); the remaining scores (our methods) are obtained using their data split.

Method	Adult	Default	Shoppers	Magic	Beijing	News	Average
SMOTE (our reproduction)	1.63 (2.55)	1.70 (1.49)	2.66 (2.16)	1.37 (1.93)	2.10 (1.62)	5.47 (3.18)	2.49 (1.75)
CTGAN	16.84 (26.31)	16.83 (14.76)	21.15 (17.20)	9.81 (13.82)	21.39 (16.45)	16.09 (9.35)	17.02 (11.99)
TVAE	14.22 (22.22)	10.17 (8.92)	24.51 (19.93)	8.25 (11.62)	19.16 (14.74)	16.62 (9.66)	15.49 (10.91)
GOGGLE	16.97 (26.52)	17.02 (14.93)	22.33 (18.15)	1.90 (2.68)	16.93 (13.02)	25.32 (14.72)	16.74 (11.79)
GReaT	12.12 (18.94)	19.94 (17.49)	14.51 (11.80)	16.16 (22.76)	8.25 (6.35)	–	14.20 (10.00)
STaSy	11.29 (17.64)	5.77 (5.06)	9.37 (7.62)	6.29 (8.86)	6.71 (5.16)	6.89 (4.01)	7.72 (5.44)
CoDi	21.38 (33.41)	15.77 (13.82)	31.84 (25.89)	11.56 (16.28)	16.94 (13.03)	32.27 (18.78)	21.63 (15.23)
TabDDPM	1.75 (2.73)	1.57 (1.38)	2.72 (2.21)	1.01 (1.42)	1.30 (1.00)	78.75 (45.83)	14.52 (10.23)
TabSYN (Our reproduction)	0.64 (1.00)	1.14 (1.00)	1.23 (1.00)	0.98 (1.38)	2.79 (2.15)	1.72 (1.00)	1.42 (1.00)
PGE-TabSyn	11.21 (17.51)	7.66 (6.72)	12.98 (10.55)	1.36 (1.74)	2.65 (2.39)	18.65 (10.84)	9.08 (6.39)
CopulaDiff	2.01 (3.14)	1.47 (1.29)	2.47 (2.01)	0.94 (1.32)	2.13 (1.64)	2.44 (1.42)	1.91 (1.35)
VAESimpleKDE	3.23 (5.05)	7.72 (6.77)	6.78 (5.51)	3.12 (4.39)	7.12 (5.48)	10.03 (5.83)	6.33 (4.46)
VAETabKDE	3.80 (5.94)	5.84 (5.12)	6.31 (5.13)	0.71 (1.0)	4.94 (3.80)	4.45 (2.59)	4.34 (3.06)
simple-KDE	1.92 (3.00)	3.33 (2.92)	3.12 (2.54)	3.59 (5.06)	10.32 (7.94)	7.36 (4.28)	4.94 (3.48)
RandCoreTabKDE	1.61 (2.52)	1.76 (1.54)	2.54 (2.07)	1.01 (1.42)	1.70 (1.31)	2.59 (1.51)	1.87 (3.48)
CoreTabKDE	3.63 (5.67)	3.29 (2.89)	3.23 (2.63)	1.08 (1.52)	3.20 (2.46)	2.87 (1.67)	2.88 (2.03)
TabKDE	1.56 (2.44)	1.55 (1.36)	2.44 (1.98)	0.78 (1.1)	1.37 (1.05)	2.52 (1.47)	1.70 (1.2)

Table 18: Performance comparison on marginal distribution alignment (Error rate %) for each dataset using TabKDE model. Values are reported as mean and standard deviation over 10 repeated runs.

Metric	Adult	Default	Shoppers	Magic	Beijing	News	Average
Marginal alignment error	1.54 ± 0.03	1.53 ± 0.05	2.46 ± 0.09	0.80 ± 0.08	1.40 ± 0.04	2.53 ± 0.04	1.71 ± 0.05

Figure 8 provides a visual comparison between some representative selected real marginal distributions and those generated by TabSYN (orange) and TabKDE (green) against the real data distributions (blue). Each row shows 4 columns from a data set. For IBM data set (bottom row) we use CopulaDiff (orange) instead of TabSYN since it cannot scale to this large data set. It is apparent that TabKDE usually does as well and better than TabSYN. In particular, on numerical data (where continuous distributions are shown), TabKDE

appears to match the real data much closer, but on categorical data, and when there are spikes in numerical data, TabKDE can have a bit more error. Since the KS distance is a worst case, it is very unforgiving for such errors on discrete data, and explains why TabKDE and TabSYN appear comparable in these marginal plots, but TabSYN has consistently smaller scores in Table 17. An average error measure on on numerical data should show an advantage for TabKDE.

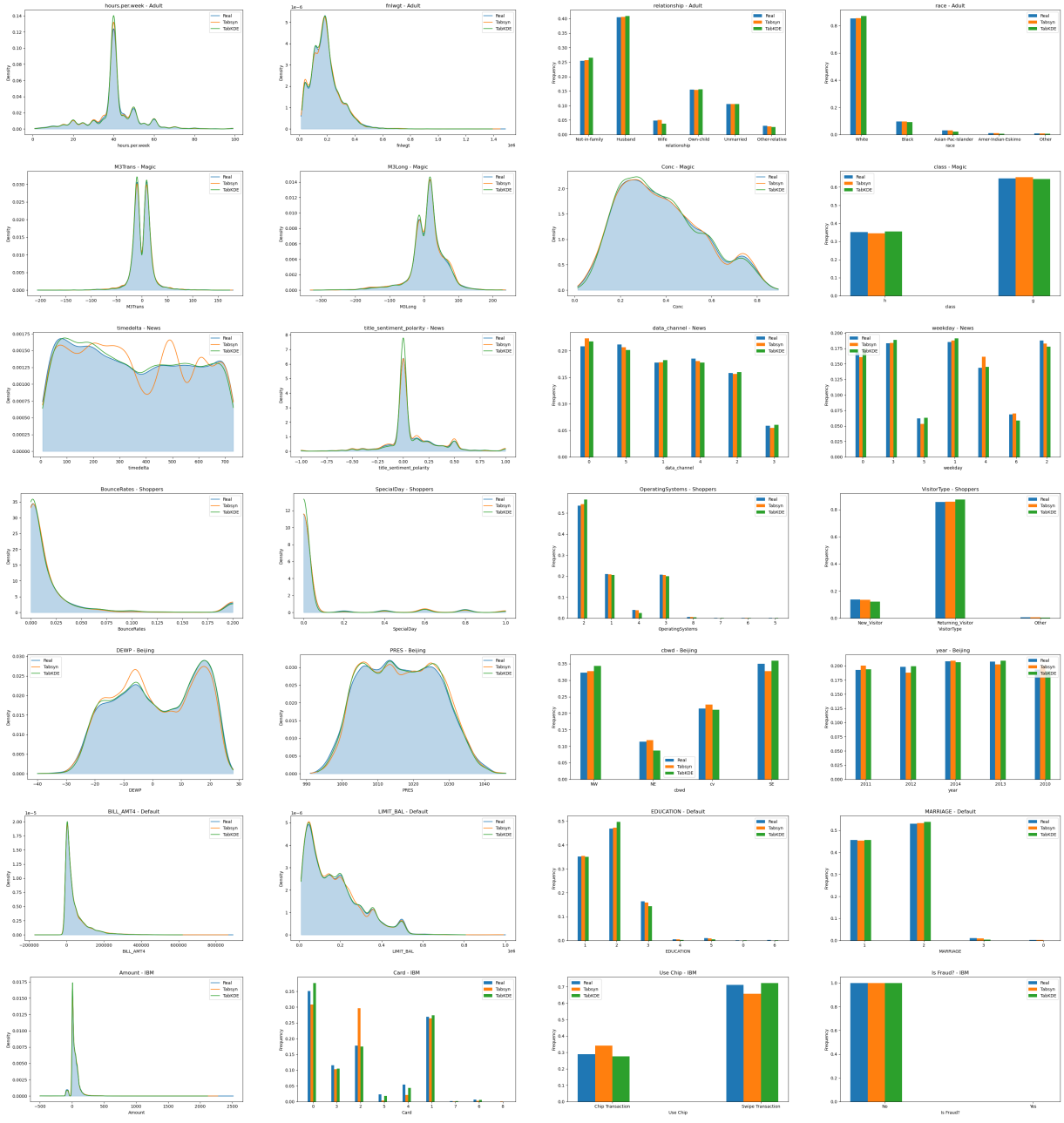

Figure 8: Marginals comparison between real data (blue), TabKDE (green), and TabSYN (orange). Each row is a data set, and sample column marginals are shown for each; some categorical and some numerical. For IBM data set (last row), TabSYN is replaced with PGE-Tabsyn since TabSYN runs out of memory.

D.2 Pairwise correlation alignment

We next measure pairwise correlation between columns. For numerical-numerical pairs, we can use standard Pearson correlations. However for pairs that involve categorical (and to align with measures in the TabSYN paper, we treat ordinal as categorical), we use contingency-table Total Variation Distances. In both metrics, smaller error values indicate that the synthetic table is more faithful to the original data. Table 19 presents, for each dataset, the average pairwise correlation alignment errors, computed as $(1 - \text{score})$, across all features for each method. A heatmap visualization of the divergence between the pairwise correlations in the real and synthetic data is presented in Figure 9. Table 20 presents the performance of the TabKDE model in Pairwise correlation alignment error (Error rate %), averaged over 10 runs.

We observe that TabKDE has better pairwise correlation alignment than all methods except TabSYN, and is comparable to SMOTE; both TabKDE and SMOTE have about 2.5 the correlation discrepancy as TabSYN. The main poor correlation for TabKDE appears in Default data set, and with 'BILL_AMT3' and 'BILL_AMT4' variables which have similar but less challenges for TabSYN, as well as GreaT and CoDi.

Table 19: Performance comparison of tabular data synthesis methods based on Pairwise correlation alignment error (Error rate %). Lower values indicate better performance. The values in parentheses denote the ratio relative to the smallest value. Baseline values, unless stated otherwise, are taken from (Zhang et al., 2024); the remaining scores (our methods) are obtained using their data split.

Method	Adult	Default	Shoppers	Magic	Beijing	News	Average
SMOTE (Our reproduction)	4.3 (2.67)	11.54 (5.11)	3.68 (1.47)	1.88 (2.29)	3.3 (1.22)	1.67 (1.25)	4.39 (1.99)
CTGAN	20.23 (12.57)	26.95 (11.92)	13.08 (5.23)	7.0 (8.54)	22.95 (8.47)	5.37 (4.01)	15.93 (7.21)
TVAE	14.15 (8.79)	19.5 (8.63)	18.67 (7.47)	5.82 (7.10)	18.01 (6.65)	6.17 (4.60)	13.72 (6.21)
GOGGLE	45.29 (28.13)	21.94 (9.71)	23.9 (9.56)	9.47 (11.55)	45.94 (16.95)	23.19 (17.31)	28.29 (12.8)
GReaT	17.59 (10.93)	70.02 (30.98)	45.16 (18.06)	10.23 (12.48)	59.6 (21.99)	–	40.52 (18.33)
STaSy	14.51 (9.01)	5.96 (2.64)	8.49 (3.39)	6.61 (8.05)	8.0 (2.96)	3.07 (2.29)	7.77 (3.52)
CoDi	22.49 (13.98)	68.41 (30.27)	17.78 (7.11)	6.53 (7.97)	7.07 (2.61)	11.1 (8.28)	22.23 (10.06)
TabDDPM	3.01 (1.87)	4.89 (2.16)	6.61 (2.64)	1.7 (2.07)	2.71 (1.00)	13.16 (9.82)	5.34 (2.42)
TabSYN(Our reproduction)	1.61 (1.00)	2.26 (1.00)	2.5 (1.00)	0.82 (1.00)	4.7 (1.73)	1.34 (1.00)	2.21 (1.00)
PGE-TabSyn	7.14 (4.43)	15.19 (6.72)	7.56 (3.02)	2.67 (2.76)	3.49 (1.29)	4.60 (3.42)	6.78 (3.07)
CopulaDiff	4.61 (2.86)	3.29 (1.46)	5.3 (2.12)	1.72 (2.10)	4.5 (1.66)	2.1 (1.57)	3.59 (1.62)
VAESimpleKDE	9.86 (6.12)	12.88 (5.70)	9.51 (3.80)	3.12 (3.80)	11.51 (4.25)	4.05 (3.02)	8.49 (3.84)
VAETabKDE	7.23 (4.49)	12.71 (5.62)	9.68 (3.87)	3.95 (4.82)	9.87 (3.64)	3.67 (2.74)	7.85 (3.55)
simple-KDE	4.64 (2.88)	5.16 (2.28)	5.26 (2.10)	3.3 (4.02)	4.72 (1.74)	2.96 (2.21)	4.34 (1.96)
RandCoreTabKDE	3.93 (2.44)	13.66 (6.04)	4.27 (1.71)	4.76 (5.80)	4.05 (1.49)	2.61 (1.95)	5.46 (2.47)
CoreTabKDE	6.3 (3.91)	9.91 (4.39)	5.77 (2.31)	2.18 (2.66)	5.86 (2.16)	2.82 (2.10)	5.47 (2.48)
TabKDE	4.51 (2.80)	9.93 (4.40)	4.31 (1.72)	2.72 (3.32)	3.74 (1.38)	2.83 (2.11)	4.67 (2.11)

Table 20: Performance comparison on pairwise correlation alignment (Error rate %) for each dataset using TabKDE model. Values are reported as mean and standard deviation over 10 repeated runs.

Metric	Adult	Default	Shoppers	Magic	Beijing	News	Average
Pairwise Corr. Error	$4.05_{\pm 0.27}$	$11.33_{\pm 1.49}$	$4.39_{\pm 0.16}$	$2.80_{\pm 0.68}$	$3.80_{\pm 0.22}$	$2.95_{\pm 0.17}$	$4.89_{\pm 0.47}$

~~We also compare against some variants on the larger IBM dataset. Recall that on our laptop CPU, neither TabSYN or SMOTE can run on this data set – they both run out of memory. Instead we compare TabKDE against our baselines including CopulaDiff and PGE-TabSyn. Also, note that we apply a modeling trick with Zip / Merchant State / Merchant City and with MCC / Merchant Name with TabKDE but not PGE-TabSyn and TabSYN (on GPU). Recall also that TabKDE (about 10 minutes training time on CPU; 40 seconds on GPU) was much faster than either of CopulaDiff (about 15 hours on CPU), PGE-TabSyn (over 40 hours on CPU) or TabSYN (OOM on CPU, about 20 minutes on GPU). The average pairwise correlation alignment error for TabSYN and PGE-TabSyn (without modeling trick) are %40.42 and %30.53, respectively, while for TabKDE and CopulaDiff (with modeling trick), are is %25.29 and %22.59; see Table 21. Indeed as shown in Figure 10 of pairwise correlation plots, the methods work largely similar except on the highly correlated pairs where we employ the modeling trick.~~It is moved to main part

Figure 9: Pairwise correlation Divergence plots for each dataset and methods.

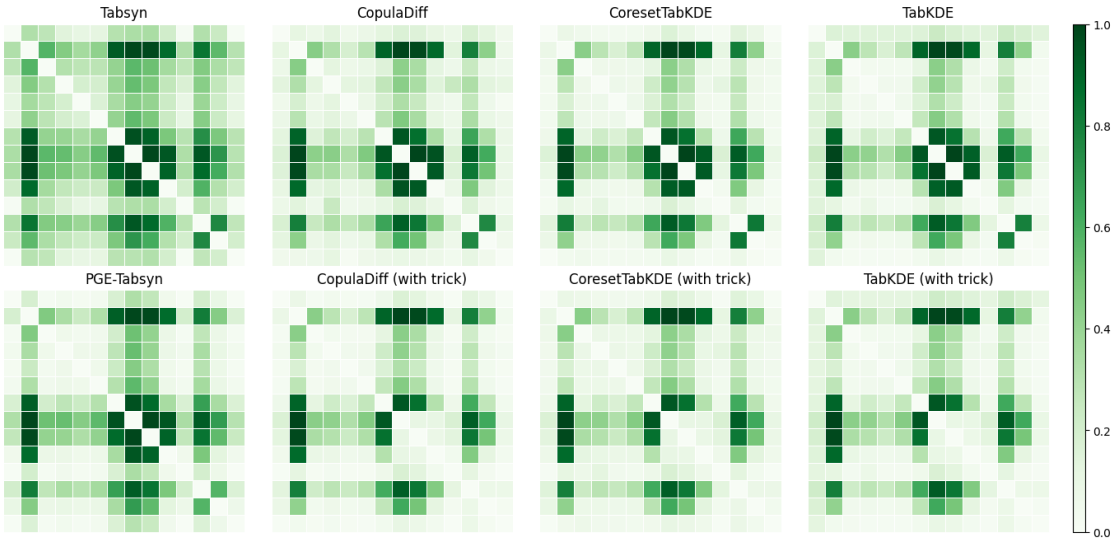

Figure 10: ~~Pairwise correlation Divergence plots for IBM dataset and methods: TabSYN (without modeling trick), PGE-Tabsyn (without modeling trick), CopulaDiff (with and without modeling trick), CoreTabKDE, TabKDE (with and without modeling trick). For CoreTabKDE, the size of coreset and the bandwidth are 5,000 and .15, respectively. Models that use the reduced modeling trick are indicated by "with trick" in parentheses.~~ It is moved to main part

Table 21: ~~Marginal and Pairwise accuracy on IBM dataset. See the last paragraph of Subsection B.1 for reduced modeling explanation.~~ It is moved to main part

Method	Marginal Alig. Error	Pairwise Corr. Error	Reduced Modeling
TabSYN	16.99	40.42	no
PGE-TabSYN	9.29	30.53	no
CopulaDiff	6.81	29.42	no
TabKDE	5.36	27.56	no
CopulaDiff	3.59	22.59	yes
CoreTabKDE	5.25	23.93	yes
TabKDE	3.58	25.29	yes

D.3 Global Distribution Alignment

High-quality synthetic data should be able to take the place of real data, letting us train models on it for downstream tasks like classification or regression and have indistinguishable performance (and without revealing private information). We assess by building a classifier to attempt to distinguish between the synthetic data and a split of data holdout from the training process. We consider two standard classifiers: XGBoost () and logistic regression.

First, following standard practice, we use XGBoost to build a classifier on the synthetic data, and measure the AUC for classification tasks, and RMSE for regression tasks. This is referred to as *machine learning efficiency*. The results in Table 22 on baselines from the TabSYN paper, as well as SMOTE, and other baselines in our model. Note that TabSYN appears twice in this table (as well as in Tables 24 and 27), to include the value recorded in Zhang et al. (2024) and then our reproduction of the result. The Real row in Table 22 shows the ideal performance, using true training data to train the classifier or regression models. The Average Gap column indicates the percentage drop in performance when synthetic data is used to train the classifier or regression models. Table 23 presents the mean and standard deviation of machine learning efficiency (MLE) over 10 runs, indicating that the TabKDE model demonstrates strong robustness with respect to this metric.

Again TabSYN provides the best error, and TabKDE is nearly as good – almost within the natural variation in TabSYN's performance. Perhaps surprisingly, the simple method smote also performs on par with TabSYN and TabKDE.

Second, we use a logistic regression classifier. Follow standard practice we now use this to try to separate the synthetic data from the heldout data. We quantify this as a classifier two-sample test (C2ST) as provided by SDMetrics; larger values closer to 1 are better. Table 24 shows both a comparison drawn directly from the TabSYN paper against a variety of recent baselines; below the line we reproduce results on TabSYN, show results for smote, and variants of our method TabKDE.

As before, TabKDE is roughly the same as SMOTE with 0.93 and only bested by TabSYN which has about 0.97. Other baselines achieve 0.79 (TabDDPM) or below 0.66.

D.4 Precision and Recall

α-Precision and β-Recall are two complementary metrics used to assess the quality of synthetic tabular data, as used in the TabSYN paper (Zhang et al., 2024). α-Precision measures the fidelity of the synthetic data to the real data, indicating how well the synthetic samples preserve fine-grained details and local structures. A higher α-Precision score reflects greater similarity to the original data. In contrast, β-Recall evaluates the extent to which the synthetic data covers the real data distribution, with higher scores indicating broader and more diverse coverage of the feature space. An ideal generative model should balance both metrics—achieving high α-Precision while also maintaining strong β-Recall—thus producing synthetic data that is both accurate and representative of the true distribution. Tables 25 and 26 summarize α-Precision and β-Recall scores.

Table 22: Machine learning efficiency performance comparison across datasets. Unless noted otherwise, scores above the line are taken from Zhang et al. (2024); the remaining scores (our methods) are obtained using their data split. To compute the Average Gap, we take the average across all datasets of the relative difference between the performance of a model trained on synthetic data (s_i) and the performance of the same model trained on real data (r_i); Average Gap $= \frac{1}{N}\sum_{i=1}^{N}\left(\frac{|s_i - r_i|}{r_i}\right) \times 100$.

Methods	**Adult** (AUC↑)	**Default** (AUC↑)	**Shoppers** (AUC↑)	**Magic** (AUC↑)	**Beijing** (RMSE↓)	**News** (RMSE↓)	**Average Gap** (%)
Real	0.927	0.770	0.926	0.946	0.423	0.842	0%
SMOTE	0.899	0.741	0.911	0.934	0.593	0.897	9.39%
CTGAN	0.886	0.696	0.875	0.855	0.902	0.880	24.5%
TVAE	0.878	0.724	0.871	0.887	.770	1.01	20.9%
GOGGLE	0.778	0.584	0.658	0.654	1.09	0.877	43.6%
GReaT	0.913	0.755	0.902	0.888	0.653	OOM	13.3%
STaSy	0.906	0.752	0.914	0.934	0.656	0.871	10.9%
CoDi	0.871	0.525	0.865	0.932	0.818	1.21	30.5%
TabDDPM	0.907	0.758	0.918	0.935	0.592	4.86	9.14%
TabSYN(Our reproduction)	0.911	0.760	0.913	0.942	0.663	0.820	10.70%
PGE-TabSyn	0.910	0.740	0.913	0.939	0.642	2.240	37.61%
CopulaDiff	0.901	0.763	0.912	0.939	0.667	0.921	12.18%
VAESimpleKDE	0.896	0.733	0.874	0.912	0.777	1.037	20.70%
VAETabKDE	0.890	0.747	0.871	0.913	0.649	0.860	11.20%
simple-KDE	0.901	0.730	0.913	0.931	0.756	1.167	21.39%
RandCoreTabKDE	0.883	0.730	0.911	0.929	0.713	0.881	14.42%
CoreTabKDE	0.881	0.712	0.919	0.928	0.744	0.877	15.86%
TabKDE	0.906	0.745	0.917	0.934	0.675	0.869	11.76%

Table 23: Machine learning efficiency comparison across datasets for the TabKDE model, reporting accuracy as mean ± standard deviation over 10 runs.

	Adult	**Default**	**Shoppers**	**Magic**	**Beijing**	**News**
MLE	0.904 ± 0.003	0.744 ± 0.012	0.916 ± 0.006	0.931 ± 0.004	0.678 ± 0.010	0.852 ± 0.021

TabSYN does the best on α-precision, but SMOTE does better on β-recall. On α-precision TabKDE (95%) nearly matches TabSYN (98.7%), and is better than any other method (including SMOTE), except our variant CopulaDiff which reaches (96%). On β-precision, TabKDE (42%) almost matches TabSYN (48%) as is almost as good as any other method with GReaT and STaSy slightly better (43%); other than SMOTE (78%). But as we discuss next, this likely because SMOTE generates data mirroring some of the training data.

E Privacy Preservation

Finally, we evaluate how well we can preserve the privacy of the training data in the synthetic data generation process. We use the distance to closest record (DCR) function in the latent space to evaluate this. That is for each synthetic data point generated, we both look at the distribution of distances to training or held-out data, and also whether the closest record was from the held-out or training set. An ideal synthetic distribution would match the distance distribution of the training data to the heldout data, and would be roughly equally likely to be close to the heldout and training data.

First Table 27 we calculate the "DCR score" which is the percentage of synthetic data closer to training data than held-out; ideally we would like this to be close to 50%. This was proposed by the recent TabDiff paper (Shi et al., 2025), and we reproduce their results in the top half of the table, and show our methods (and SMOTE and TabSYN) below the line on an equal split. We see most diffusion methods (including our

Table 24: C2ST Scores of generative models on tabular datasets. Unless noted otherwise, scores above the line are taken from Zhang et al. (2024); the remaining scores (our methods) are obtained using their data split.

Method	Adult	Default	Shoppers	Magic	Beijing	News	Average
SMOTE(Our reproduction)	0.9212	0.9332	0.9107	0.9803	0.9972	0.8633	0.9334
CTGAN	0.5949	0.4875	0.7488	0.6728	0.7531	0.6947	0.6586
TVAE	0.6315	0.6547	0.2962	0.7706	0.8659	0.4076	0.6044
GOGGLE	0.1114	0.5163	0.1418	0.3262	0.4779	0.0745	0.2747
GReaT	0.5376	0.4710	0.4285	0.4326	0.6893	—	0.5118
STaSy	0.4054	0.6814	0.5482	0.6939	0.7922	0.5287	0.6083
CoDi	0.2077	0.4595	0.2784	0.7206	0.7177	0.0201	0.4007
TabDDPM	0.9755	0.9712	0.8349	0.9998	0.9513	0.0002	0.7888
TabSYN(Our reproduction)	0.9949	0.9804	0.9699	0.9893	0.9268	0.9584	0.9699
PGE-TabSyn	0.9240	0.9039	0.7679	0.9859	0.8629	0.8060	0.8751
CopulaDiff	0.8557	0.9798	0.8665	0.9914	0.9576	0.9793	0.9384
VAESimpleKDE	0.7199	0.4082	0.6736	0.9665	0.7392	0.3782	0.6476
VAETabKDE	0.7483	0.4828	0.7242	0.9984	0.8022	0.8075	0.7606
simple-KDE	0.9196	0.8716	0.8110	0.9711	0.9497	0.4975	0.8368
RandCoreTabKDE	0.9215	0.9570	0.8757	0.9921	0.9503	0.8901	0.9311
CoreTabKDE	0.8254	0.873	0.8462	0.9864	0.8924	0.8643	0.8813
TabKDE	0.9219	0.9579	0.9161	1.0000	0.9514	0.8819	0.9382

Table 25: α-Precision scores for various methods on the 6 standard data sets. The last column shows the average score and rank. Unless noted otherwise, scores above the line are taken from Zhang et al. (2024); the remaining scores (our methods) are obtained using their data split.

Method	Adult	Default	Shoppers	Magic	Beijing	News	Average	Ranking
SMOTE(Our reproduction)	92.83	98.40	92.60	96.76	98.64	87.93	94.52	6
CTGAN	77.74	62.08	76.97	86.90	96.27	96.96	82.82	12
TVAE	98.17	85.57	58.19	86.19	97.20	86.41	85.29	10
GOGGLE	50.68	68.89	86.95	90.88	88.81	86.41	78.77	15
GReaT	55.79	85.90	78.88	85.46	98.32	-	80.87	13
STaSy	82.87	90.48	89.65	86.56	89.16	94.76	88.91	8
CoDi	77.58	82.38	94.95	85.01	98.13	87.15	87.03	9
TabDDPM	96.36	97.59	88.55	98.59	97.93	0.00	79.83	14
TabSYN(Our reproduction)	99.19	98.79	97.57	99.69	98.85	97.04	98.52	1
CopulaDiff	98.09	98.99	95.43	98.43	97.33	93.98	97.04	2
VAESimpleKDE	88.21	80.90	82.46	7.03	75.56	19.29	72.24	16
VAETabKDE	98.39	91.71	97.36	98.50	93.29	84.86	94.02	7
simple-KDE	98.10	93.88	98.84	90.13	96.41	29.25	84.44	11
RandCoreTabKDE	95.67	4.62	91.64	98.68	98.11	96.68	95.90	3
CoreTabKDE	98.01	89.44	90.27	99.12	95.70	94.96	94.58	5
TabKDE	94.46	94.45	92.18	98.98	97.47	97.48	95.83	4

CopulaDiff) can consistently achieve below 52%. Our main method TabKDE obtains an average DCR score of about 58%, which is servicable.

On the other hand, smote has an average DCR score of 95%. This indicates that it often nearly replicates the training data. Its method chooses a training record, finds the k nearest neighbor, and selects a new point in the convex combination of these points, then de-tokenizes back to the tabular format. Because it works

Table 26: β-Recall scores for various methods on the 6 standard data sets. The last column shows the average score and rank. Unless noted otherwise, scores above the line are taken from Zhang et al. (2024); the remaining scores (our methods) are obtained using their data split.

Method	Adult	Default	Shoppers	Magic	Beijing	News	Average	Ranking
SMOTE(Our reproduction)	76.88	76.00	77.09	82.45	79.22	80.00	78.60	1
CTGAN	30.80	18.22	31.80	11.75	34.80	24.97	25.39	16
TVAE	38.87	23.13	19.78	32.44	28.45	29.66	28.72	15
GOGGLE	8.80	14.38	9.79	9.88	19.87	2.03	10.79	17
GReaT	49.12	42.04	44.90	34.91	43.34	OOM	42.86	6
STaSy	29.21	39.31	37.24	53.97	54.79	39.42	42.99	5
CoDi	9.20	19.94	20.82	50.56	52.19	34.40	31.19	13
TabDDPM	47.05	47.83	47.79	48.46	56.92	0.00	41.34	7
TabSYN(Our reproduction)	47.53	46.74	48.85	47.64	50.56	45.10	47.74	2
CopulaDiff	41,29	46.21	43.21	46.38	51.65	43.86	45.43	3
VAESimpleKDE	38.78	20.71	38.01	40.13	45.62	2.00	30.87	14
VAETabKDE	43.68	27.32	48.81	45.56	51.12	12.64	38.18	9
simple-KDE	45.90	36.60	43.12	44.78	52.68	3.90	37.83	11
RandCoreTabKDE	37.67	35.81	44.77	44.82	51.56	17.54	38.69	8
CoreTabKDE	27.46	20.86	39.40	40.35	48.30	13.01	31.56	12
TabKDE	48.54	43.05	47.22	48.80	54.39	17.82	43.30	4

with a one-hot encoding, probably most records map back to the same discrete values as the first record, and it often failures to generate substantially new data, hence leaking the training data.

Table 27: The DCR score indicates the likelihood that a generated data sample resembles the training set more than the test set. A value nearer to 50% is considered ideal. Ratios recomputed using the true minimum in each column. Values above the line, unless stated otherwise, are taken from (Shi et al., 2025); the remaining scores (our methods) are obtained using their data split.

Method	Adult	Default	Shoppers	Beijing	News	Average
SMOTE(Our reproduction)	91.18 (1.83)	91.46 (1.82)	96.76 (1.93)	100.00 (1.99)	99.00 (1.96)	95.68 (1.89)
STaSy	50.33 (1.01)	50.23 (1.00)	51.53 (1.03)	50.59 (1.01)	50.59 (1.00)	50.65 (1.00)
CoDi	49.92 (1.00)	51.82 (1.03)	51.06 (1.02)	50.87 (1.01)	50.79 (1.00)	50.89 (1.01)
TabDDPM	51.14 (1.02)	52.15 (1.04)	63.23 (1.26)	80.11 (1.59)	79.31 (1.57)	65.19 (1.29)
TabSYN(Our reproduction)	51.33 (1.03)	51.61 (1.03)	51.99 (1.03)	53.20 (1.06)	50.76 (1.00)	51.78 (1.02)
TabDiff	50.10 (1.00)	51.11 (1.02)	50.24 (1.00)	50.50 (1.00)	51.04 (1.01)	50.60 (1.00)
PGE-Tabsyn	50.38 (1.01)	51.33 (1.01)	51.81 (1.03)	50.67 (1.01)	50.48 (1.00)	50.94 (1.01)
CopulaDiff	50.34 (1.01)	50.96 (1.01)	50.72 (1.01)	50.29 (1.00)	53.00 (1.05)	51.06 (1.01)
VAESimpleKDE	61.33 (1.23)	58.08 (1.16)	58.83 (1.17)	60.73 (1.21)	59.00 (1.17)	59.59 (1.18)
VAETabKDE	61.28 (1.23)	57.87 (1.15)	57.70 (1.15)	60.42 (1.20)	58.00 (1.15)	59.45 (1.17)
simple-KDE	63.32 (1.27)	63.49 (1.26)	58.18 (1.16)	55.42 (1.10)	56.12 (1.11)	59.71 (1.18)
RandCoreTabKDE	62.30 (1.25)	63.09 (1.26)	58.91 (1.17)	63.50 (1.26)	55.59 (1.10)	60.68 (1.20)
CoreTabKDE	52.59 (1.05)	54.11 (1.08)	55.04 (1.10)	51.17 (1.02)	52.00 (1.03)	52.98 (1.05)
TabKDE	62.23 (1.25)	63.46 (1.26)	58.80 (1.17)	54.24 (1.08)	54.54 (1.08)	58.55 (1.16)

If the closest record is from the training or heldout data is an imperfect measure of privacy, since there may be heldout data nearly as close. One way to evaluate this is to consider the distribution of how close the synthetic data to the heldout (red) matches the distribution of the synthetic data to the train (blue). We show this in Figure 11 for TabKDE, TabSYN, and smote for the 6 standard datasets. We observe that for TabKDE and TabSYN these distributions are multi-modal, but still match almost perfectly for each data set. On the other hand smote has a very different distribution, and the synthetic to train (blue) is always

much smaller (almost always close to 0 for Adult, Default, Shopping, and Beijing), indicating it is too closely just reproducing the training data.

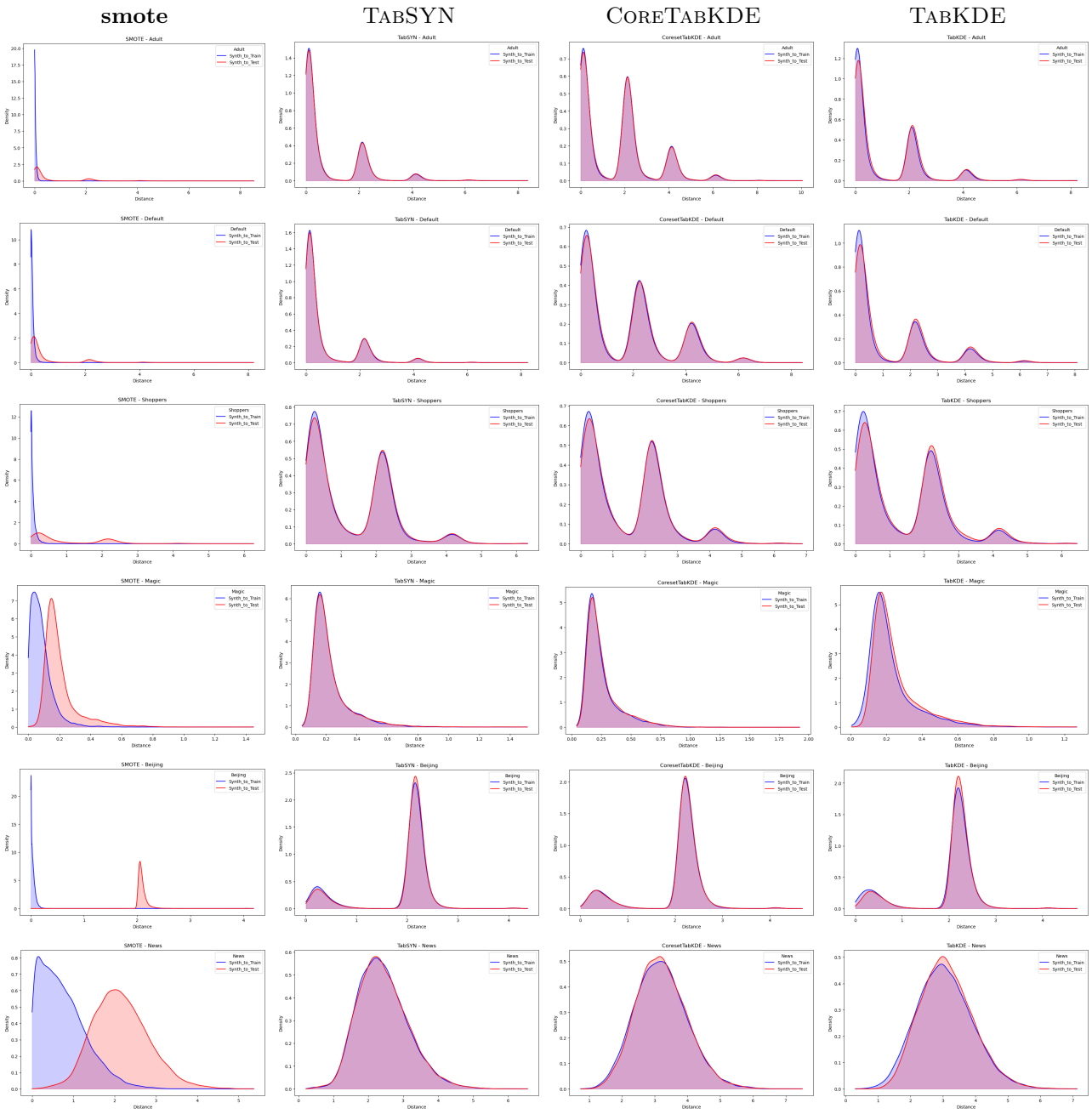

Figure 11: Privacy comparison based on DCR distributions for synthetic to training data (blue) and synthetic to held-out data (red). Each row is a data set, the columns show results for SMOTE, TabSYN, CoreTabKDE, and TabKDE.

We note a practical limitation in computing DCR for datasets with high-cardinality categorical features. In the IBM dataset, 13 categorical columns each have thousands of distinct values; under standard one-hot encoding, this yields $37,722$ dimensions. At this scale, both memory usage and computational cost become prohibitive and exceeded our available hardware, leading to out-of-memory failures during evaluation (even with aggressive use of FAISS). While dimensionality reduction could mitigate the resource burden, it would

also alter the meaning of DCR by assessing proximity in a compressed space rather than the original feature space. Accordingly, we report that DCR evaluation was not feasible for our highest-dimensional dataset under our computational constraints.

F Coresets for Generative Tabular Data Modeling

A *coreset* (Phillips, 2016) is a compact, weighted set of points that provides a close approximation to the full dataset for a specific downstream task. In the context of Kernel Density Estimation (KDE), a coreset serves to approximate the full KDE using significantly fewer, yet strategically chosen, representative points. A *weak coreset* is a coreset that the set is not necessarily a subset of the original point set. In this setting, the "weak" aspect will turn out to be strategically advantageous.

Our proposed TabKDE framework employs the full KDE to generate samples from the Copula latent representation $Z \subset [0,1]^{n \times d}$ of the tabular data $\mathcal{T}$. The full KDE over Z is given by:

$$f_Z(z) = \frac{1}{|Z|} \sum_{z_i \in Z} K\left(\frac{z - z_i}{h}\right),$$

which we here consider it as the ground-truth likelihood function over $z \in [0,1]^d$. To approximate $f_Z(\cdot)$ using a weak coreset, we define a parameterized KDE $\tilde{f}_\Theta(\cdot)$ based on a small set of learnable coreset (support) points $Q = \{q_1, \ldots, q_m\}$ and their corresponding non-negative weights $W = \{\omega_1, \ldots, \omega_m\}$, constrained such that $\sum_{i=1}^m \omega_i = 1$, where $\Theta = \{Q, W\}$. The approximated density function is:

$$\tilde{f}_\Theta(z) = \sum_{i=1}^{m} \omega_i K\left(\frac{z - q_i}{h}\right),$$

with $m \ll n$. It is known (Phillips & Tai, 2020) that a sample $Q \sim Z$ of $m = O((1/\varepsilon^2)\log(1/\delta))$ points already ensures a strong L_∞ coresets approximation that $\|f_Z - f_Q\|_\infty \leq \varepsilon$ with probability at least $1 - \delta$. Note that for a fixed kernel K, this bound is independent of the dimension d. While we use this as a starting point, we seek to improve it with a weak coreset.

In particular, the parameters Θ are optimized by minimizing the expected squared L_2 deviation between the full KDE and its coreset approximation, evaluated over samples drawn from the uniform distribution on $[0,1]^d$:

$$\mathbb{E}_{z \sim \mathsf{Unif}([0,1]^d)} \left[\left(\tilde{f}_\Theta(z) - f_Z(z) \right)^2 \right].$$

By optimizing the positions and weights of the coreset points to minimize the discrepancy between the coreset-based KDE and the full KDE, the method preserves key distributional features, such as modes, spread, and overall shape. Moreover, because we use a weak coreset, we are not replicating the training data, and this minimizes the risk of overfitting to the data or leaking its private attributes.

This objective can be optimized via stochastic gradient descent (SGD) with TrainCoresetKDE (Algorithm 14).

Algorithm 14 TrainCoresetKDE(Z, T)

Define $f_Z(z) = \frac{1}{|Z|} \sum_{z_i \in Z} K\left(\frac{z - z_i}{h}\right)$
Initialize randomly the coreset points $Q = \{q_1, \ldots, q_m\} \subset Z$
Initialize the weights $W = \{\omega_1, \ldots, \omega_m\}$ with $\omega_i = 1/m$
Define $\tilde{f}_\Theta(z) = \sum_{i=1}^m \omega_i K\left(\frac{z - q_i}{h}\right)$
For $t = 1$ to T:
    Sample $z \sim \mathsf{Unif}([0,1]^d)$
    Compute loss $\mathcal{L}(z) = \left(\tilde{f}_\Theta(z) - f(z)\right)^2$
    Update Θ via gradient descent to minimize $\mathcal{L}(z)$
return $\Theta = \{Q, W\}$

We employ the Gaussian kernel as $K(v) = \exp(-v^2)$ in our formulation. Once trained, the learned weak coreset $\{(q_i, \omega_i)\}_{i=1}^m$ replaces the full KDE sampling step in Algorithm 11. This modification constitutes the only difference between TabKDE and CoresetTabKDE, and is detailed in the sampling procedure below.

Algorithm 15 SampleCoresetKDE-iterative(Q, W)

$Q, W =$ TrainCoresetKDE(Z, T)
Sample $q_i \in Q$ with probability $\omega_i \in W$
Sample radius $r > 0$ from f
Sample $v \sim \mathcal{N}(0, \Sigma)$, set $u = \frac{v}{\|v\|}$
$z' \leftarrow z_i + r \cdot u$
While $\{j : z'_j \notin [0,1]\} \neq \varnothing$:
    $J \leftarrow \{j : z'_j \notin [0,1]\}$
    Sample $v' \sim \mathcal{N}(0, \Sigma)$, set $w = \frac{v'}{\|v'\|}$
    $s \leftarrow \frac{\|(u_k)_{k \in J}\|}{\|(w_k)_{k \in J}\|}$
    $u_j \leftarrow s \cdot w_j$ for each $j \in J$
    $z' \leftarrow z_i + r \cdot u$
return z'

We may also define a RandomCoresetTabKDE variant, in which the optimization step in Alg. 14 (Step 1) is omitted. Instead, a subset $Q \subset Z$ of size m is sampled uniformly at random; then we simply invoke SampleKDE-iterative(Q) (Alg 11) with Q instead of Z. As noted above, this simple approach of taking a random sample $Q \sim Z$ has strong L_∞ approximation guarantees on how well it approximates the KDE of Z; and this does not depend on either the dimension d or the size n of Z – it only depends on the size $|Q| = m$ of the sample.

F.1 Empirical Evaluation of Coreset Methods

In this section, we empirically examine the advantages and limitations of the coreset approaches CoreTabKDE and RandCoreTabKDE introduced in Subsection F. Across all the data sets, we set $m = 5{,}000$; as shown in Figure 12, the marginal and pairwise correlation alignment scores look to plateau around that value. By ablation study, we set $h = 0.2$ for data sets Adult, Default, Shoppers, Magic, Beijing, and News, we set $h = 0.2, 0.4, 0.2, 0.2, 0.2, 0.5$, respectively. We consider bandwidths $h \in \{0.1, 0.2, \ldots, 1.0\}$ at 0.1 intervals, and examine the loss function of the TrainCoresetKDE procedure run for $T = 30$ epochs. We select the bandwidth h where the corresponding loss has the steepest descent towards zero. High values of h result in negligible loss updates, while overly small values lead to premature convergence at suboptimal loss values. If multiple consecutive bandwidths yield similar behavior, we take the smaller as the chosen value.

While the bandwidth selection is chosen based only on the loss function in the training data, we also validate our selection on the test data. As shown on the Adult data set with $m = 5000$ in Figure 13, the alignment error (both marginal and pairwise correlation; higher better) is fairly stable across choices of h in 0.1 to 1.0, but has a local peak around $h = 0.2$. Moreover, the DCR score has a more noticeable drop for $h \leq 0.6$; hence $h = 0.2$ is confirmed as a good choice. While this KDE is built in $[0,1]^d$ copula space for all data sets, the dimension changes from 6 (for Adult) to 46 (for News), and the higher dimensional setting has more room to spread points out, and prefers a larger bandwidth.

The accuracy scores are reported in the numerous tables above, and one can observe this method achieves accuracy nearly as good as TabKDE, but often a bit worse; see for instance Tables 17 and 19. The scalability of RandCoreTabKDE is also about the same on the data sets we consider as TabKDE (which is already very efficient). However, now we require much less space to store the model; and the based on KDE-coreset results (Phillips & Tai, 2020; Joshi et al., 2011), the accuracy for a fixed size coreset should not decrease as the training data grows. However, the CoreTabKDE requires some optimization training time: approximately 55 minutes (on the laptop CPU) average across the five datasets: Adult, Default, Shoppers, Magic, and Beijing.

What is more interesting is the effect on privacy in using CoreTabKDE. As shown in Table 27, CoreTabKDE offers a notable improvement in privacy (under the unstable DCR score), with an average DCR score of about 53%. This is because the coreset no longer precisely stores the training data; rather it is storing a distribution of data points Q which have a similar KDE as does the training data Z. Hence, when it generates synthetic data, it is not using some training data point $z \in Z$ as a starting point.

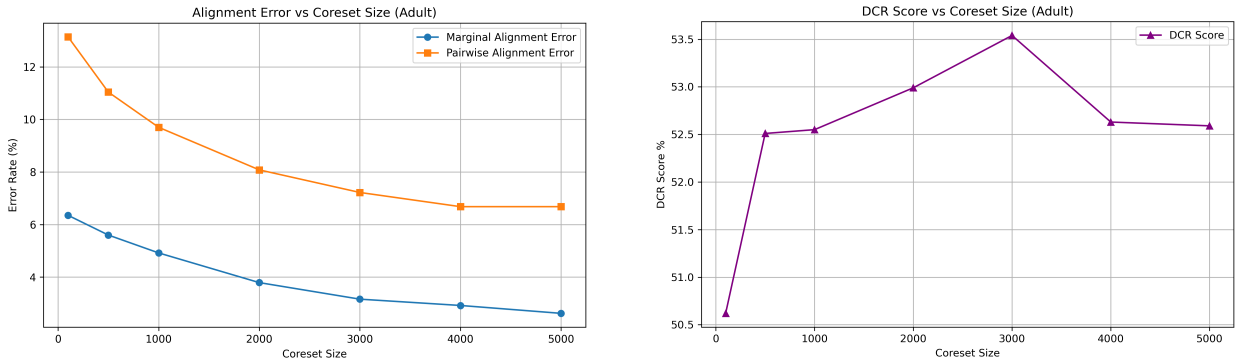

Figure 12: Left: Marginal distribution alignment error (%) and pairwise correlation alignment error (%) as coreset size increases. Right: DCR score as coreset size increases.

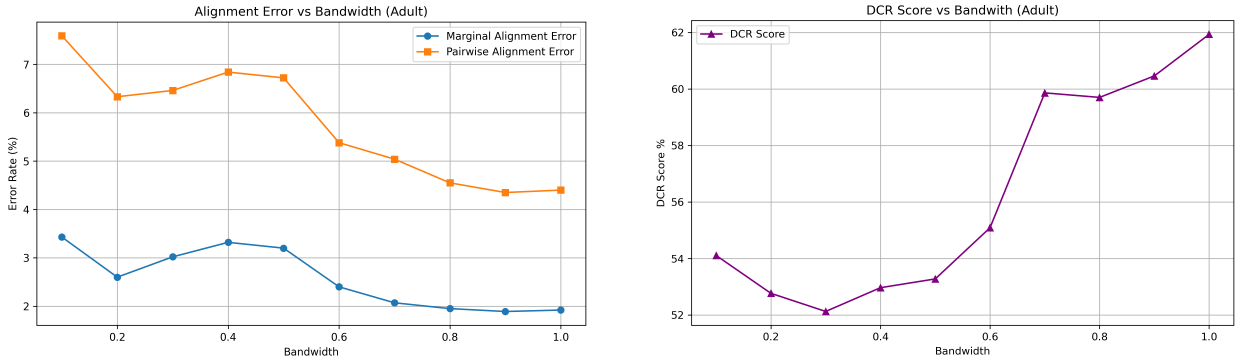

Figure 13: Left: Marginal distribution alignment error (%) and pairwise correlation alignment error (%) as bandwidth increases. Right: DCR score as bandwidth increases.

G Ablation Study on Variants of TabKDE

In this section we do a small ablation study to investigate the differences among variants of TabKDE. Most data is presented in earlier tables in the main paper. The main take-a-ways are as follows.

The methods that use Diffusion or VAE are significantly slower, and less scalable. As discussed above some of this can be ameliorated by avoiding one-hot encoding, but still the difference in runtime is very large on the IBM data set. Second, none of the methods that take elements from TabSYN directly match it in terms of accuracy, although CopulaDiff sometimes does nearly as well, and on average, they all also do not outperform TabKDE. Third, on privacy, CopulaDiff achieves an average DCR score of 51%, so it does quite well, improving upon TabKDE and CoreTabKDE.

We next provide analysis comparing to SimpleKDE. It should already have been apparent from the accuracy evaluation where it performs a bit worse than TabKDE that it is not the preferred method. But next we provide a more in depth discussion on the marginals, where the issue becomes even more clear why the iterative element is required.

G.1 Motivation for TabKDE: Boundary Control Challenges in SimpleKDE

In our initial exploration, we employed **SimpleKDE** to generate synthetic samples by perturbing numerical latent representation of the data points using a Kernel Density Estimation (KDE) model. While this approach is intuitive and straightforward, it presents a critical limitation—*lack of boundary control* (see Figure 14). The perturbed samples, generated by adding Gaussian noise to real points, often fall outside the convex hull of the original dataset. This results in synthetic records that do not reflect the valid range or domain constraints of the original data, leading to unrealistic samples that may violate the natural boundaries of the feature space.

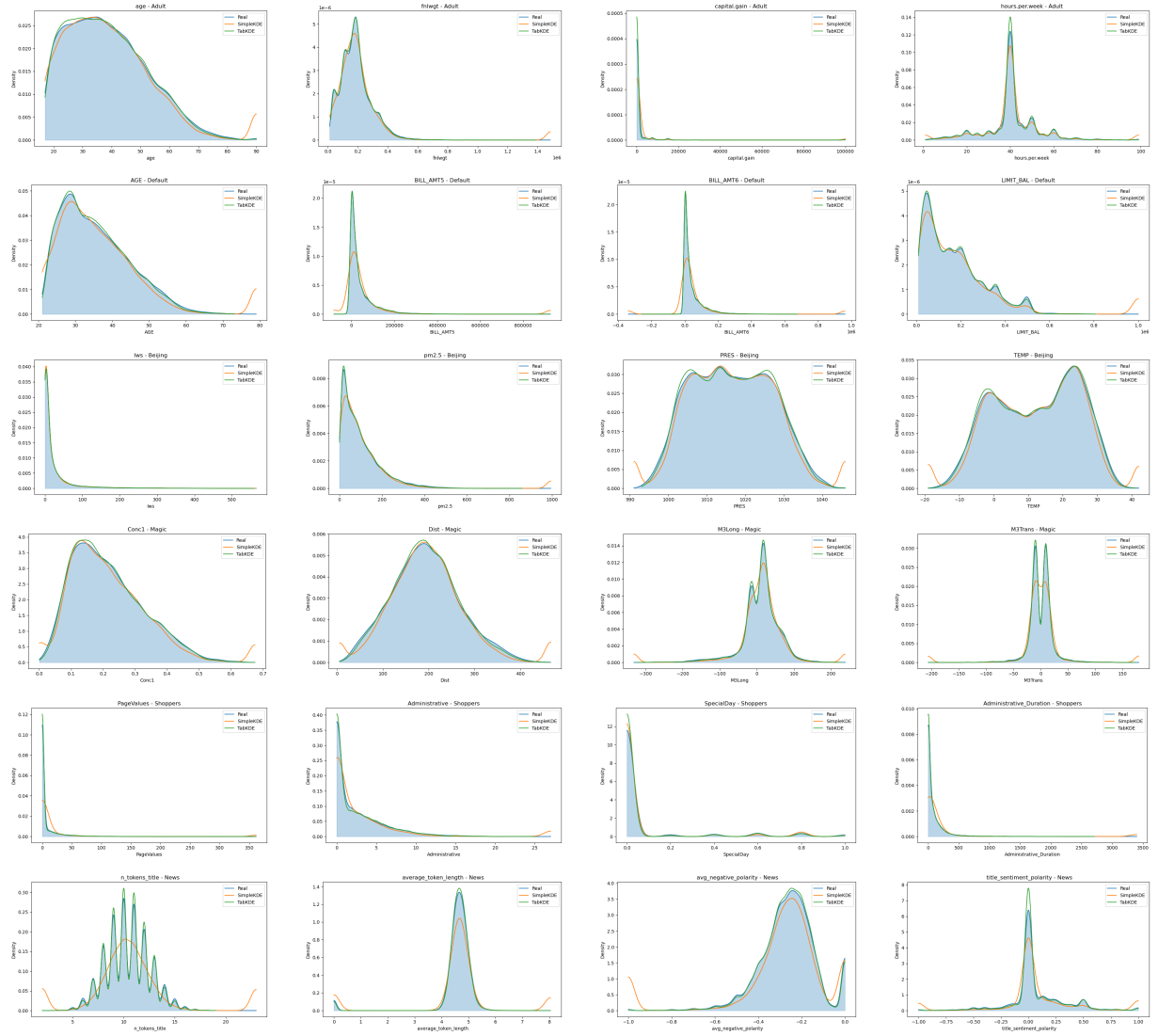

Figure 14: Marginals comparison: Simple KDE vs TabKDE

To address this issue, we developed TabKDE to better leverage the copula-transformed latent space, where all features reside. We ensure effective boundary control during sampling, maintaining the generated samples within valid limits. By resolving the boundary control problem, TabKDE produces synthetic data that more accurately preserves the statistical structure and integrity of the original dataset (see Figure 14).

G.2 Statistic on boundary correction in TabKDE

As discussed in Section 2.4, we employ a boundary-aware sampler to avoid out-of-boundary samples. Table 28 reports an ablation of boundary correction behavior across datasets, including the average and maximum number of coordinate resampling iterations, as well as the number of sampling failures, defined as cases where some coordinates remain out of bounds after $10 \times d$ resampling attempts. We refer the reader to Appendix B.1 for a description of the IBM datasets with and without the modeling trick.

Across all datasets, boundary correction is rarely needed: the mean number of coordinate-resampling iterations (denoted "Correction iterations" in Table 28) below 1 for every dataset except News, indicating that most sampled coordinates fall within valid bounds on the first draw. Even when correction is required, it remains modest–the maximum number of iterations is at most 9 across datasets (excluding 1 failure in News dataset out of the 35679 samples we generate), suggesting fast convergence of the boundary-aware sampler. Sampling failures are essentially absent: we observe zero failures on all datasets except News, which exhibits a single failure under the $10 \times d$ resampling budget. For the IBM datasets, the modeling trick reduces the correction burden (mean iterations $0.81 \rightarrow 0.58$ and max iterations $8 \rightarrow 6$) which is expected since the dimension is decreased from 14 to 11 due to the modeling trick.

Table 28: Boundary-correction statistics for the boundary-aware sampler used in TabKDE. For each dataset, we report the mean $\pm$ standard deviation of the number of coordinate-resampling iterations required to obtain an in-bounds sample, the maximum number of iterations observed (for successful samples), and the number of sampling failures (coordinates still out of bounds after $10 \times d$ resampling attempts).

Dataset	Size	Features	Correction iterations	Max iterations	Failed
Adult	32561	15	0.30 $\pm$ 0.52	4	0
Default	27000	24	0.64 $\pm$ 0.74	9	0
Shoppers	11097	18	0.55 $\pm$ 0.65	5	0
Magic	17117	11	0.38 $\pm$ 0.64	7	0
Beijing	37581	12	0.36 $\pm$ 0.56	6	0
News	35679	48	1.74 $\pm$ 0.83	8	1
IBM(no trick)	176221	14	0.81 $\pm$ 0.69	8	0
IBM(w/ trick)	176221	11	0.58 $\pm$ 0.63	6	0

H Comparison with Copula/KDE Based generator Models

Copula-based models represent one of the earliest and most widely used approaches for synthetic tabular data generation. These methods typically rely on two steps: (i) learning marginal distributions for each feature, and (ii) coupling them via a copula function to capture dependencies across variables. Classic examples include the *GaussianCopulaSynthesizer* (Patki et al., 2016), which estimates univariate marginals and applies a Gaussian copula to model correlations, and its variants such as *CopulaGAN* and vine-copula GANs, which map the copula-transformed data into a latent space before adversarial training (Xu et al., 2019). While conceptually elegant, these methods often struggle with mixed-type tabular data. Categorical variables are usually handled by simplistic encodings (e.g., one-hot encoding or UniformEncoder), which can distort dependencies, and the Gaussian copula assumption may fail to capture higher-order interactions.

Recent research has extended this line of work. For example, (Meyer et al., 2021) applied vine and Gaussian copulas to continuous weather data, while (Majdara & Nooshabadi, 2020) integrated copula transforms with diffusion-based KDE for continuous density estimation. However, these methods are limited to continuous domains and do not address challenges of mixed categorical-numerical data or scalability. Other work, such as differentially private copula models (e.g., (Gambs et al., 2021)), explicitly aims to strengthen privacy at the expense of accuracy and efficiency.

Against this backdrop, TabKDE can be viewed as both building on and diverging from the copula tradition. Like classical copula generators, TabKDE maps data into a copula space (not the same as the classical copula method), standardizing marginals into the unit hypercube. However, rather than imposing parametric assumptions (e.g., Gaussian copula) or adversarial training, it employs a d-dimensional kernel density estimator directly in copula space. This design introduces several key innovations absent from prior copula models:

- **Principal-Guided Encoding (PGE)** for categorical features, enabling faithful one-dimensional embeddings without using one-hot encodings, which does not increase the dimension and avoids sparsity.

- **Covariance-aware geometry and boundary-respecting kernels**, which allow KDE sampling to preserve higher-order correlations and respect marginal supports.

- **DCR-calibrated kernels**, which explicitly align synthetic samples to the empirical distance-to-closest-record distribution, thereby privacy protection.

- **Coreset compression**, which produces compact, scalable generative models, in contrast to copula baselines that typically scale linearly with dataset size.

Empirical comparisons reinforce these differences. Across UCI benchmarks (Adult, Default, Magic,) and a large IBM fraud dataset, TabKDE consistently achieves lower marginal and pairwise correlation errors and substantially higher C2ST fidelity than GaussianCopulaSynthesizer, while also surpassing CopulaGAN in distributional accuracy. GaussianCopulaSynthesizer maintains slightly stronger privacy under the DCR metric (hovering near the ideal 50%), but this advantage stems largely from its poorer fidelity. In practice, TabKDE achieves a more balanced tradeoff: reasonable privacy coupled with diffusion-level accuracy, while retaining orders-of-magnitude efficiency gains, training in minutes compared to hours for deep copula-hybrids like CopulaGAN.

To further contextualize our approach, we compare TabKDE against both the classical *GaussianCopulaSynthesizer* and *CopulaGANSynthesizer*, in addition to our CopulaDiff variant. Table 29 reports averages across Adult, Default, Shoppers, Beijing, and News, while Tables 30 provide per-dataset breakdowns for Adult, Default, Magic, and Beijing.

Metric (↓ better except C2ST ↑)	**TabKDE**	**CopulaDiff**	**GaussianCopula**
Average Marginal error (%)	**1.70**	1.91	14.9
Average Pairwise-corr error (%)	4.67	**3.59**	13.3
Average C2ST (↑)	**0.94**	**0.94**	0.22
DCR (ideal ≈ 50%)	58.6	51.06	**49.8**
Train / Sample time (s, CPU)	39.2 / 39.0	–	**0.9 / 6.8**

Table 29: Comparison of TabKDE and CopulaDiff against the GaussianCopulaSynthesizer. Averages are computed over Adult, Default, Shoppers, Beijing, and News datasets.

Accuracy. TabKDE achieves 7–10× lower distribution-alignment errors and quadruples C2ST fidelity compared to the GaussianCopulaSynthesizer. This indicates that our encoding of the copula transform together with the KDE estimator drives the observed accuracy gains.

Speed. GaussianCopulaSynthesizer is milliseconds-fast on CPU, effectively functioning as a restricted subset of TabKDE. Nonetheless, TabKDE remains far more efficient than deep generative models.

Privacy. GaussianCopulaSynthesizer yields DCR scores near the ideal 50%, reflecting strong privacy but poor fidelity. TabKDE (58%) attains a more balanced trade-off, offering reasonable privacy while maintaining high fidelity. Note that DCR is an imperfect metric: it only evaluates nearest-neighbor distances, and broader distributional comparisons are more favorable for TabKDE.

Overall, TabKDE consistently outperforms both complex copula-based generators (e.g., CopulaGAN) and the simpler GaussianCopula model in terms of fidelity, while remaining efficient and maintaining reasonable privacy.

H.1 Extended Copula+KDE Baselines

We additionally benchmark TabKDE against several methods at the intersection of copulas and kernel density estimation (KDE). These include existing implementations in SDV and baselines we constructed, along with a differentially private Gaussian Copula model.

Copula+KDE Baselines. The comparison space includes a variety of copula-based and KDE-based extensions. Tables 30 present results on the Adult, Default, Magic, and Beijing datasets.

CopulaGAN applies an empirical copula transform followed by GAN-based generation, while GaussianCopula also relies on the copula transform but pairs it with Gaussian marginals. The GaussianKDECopulaSynthesizer, implemented in SDV with `default_distribution="gaussian_kde"`, fits Gaussian KDEs on marginals but is extremely slow in practice, requiring about 2.5 hours compared to roughly one minute for TabKDE. We also construct a CopulaKDE baseline, which uses an empirical copula transform followed by a d-dimensional Gaussian KDE in latent space $[0,1]^d$ with the bandwidth σ set to the median pairwise distance.

Below the lines in Tables 30 are our variants. CopulaDiff represents our diffusion-based variant applied after a copula transform. SimpleKDE is a variant of TabKDE that incorporates a DCR-calibrated kernel and covariance-aware directions, but omits boundary-aware sampling. Finally, TabKDE is our proposed method.

Three central observations arise from the experiments. In terms of accuracy, TabKDE consistently achieves the best or near-best fidelity. While some competitors such as CopulaDiff, SimpleKDE, or GaussianKDECopula perform strongly on C2ST, they typically fall short in marginal or pairwise errors. Regarding privacy, the SDV copula models and the DP Gaussian Copula reach DCR values close to the ideal 50%, but they incur substantially higher errors. As expected, stronger privacy guarantees correlate with reduced fidelity. TabKDE offers a balanced tradeoff, maintaining high fidelity while still achieving moderate privacy with DCR around 58%. Finally, in terms of scalability, GaussianKDECopulaSynthesizer is prohibitively slow, taking several hours compared to TabKDE's single-minute runtime. TabKDE thus emerges as both more efficient and more accurate.

H.2 Differentially Private Gaussian Copula

In addition to the above, we benchmark a differentially private (DP) Gaussian Copula model with a specified privacy budget ϵ. Table 31 reports the results.

Note that while this achieves strong DCR score (as do similar copula methods without DP guarantees), there is not a clear advantage as the ϵ parameter is decreased. However, the resulting Marginal Error (about 17%) and Pairwise Correlation (about 28%) scores are significantly higher than most other baselines; TabKDE achieves 1.56% and 4.51%. Also C2ST (about 0.35) is worse that most baselines; TabKDE achieves 0.92, where higher is better.

So while this method does provide a DP guarantee, it appears to perform significantly worse in all accuracy measures, even for very large ϵ values.

Adult	Marginal Err. (↓)	Pairwise Corr. (↓)	DCR (→ 50)	C2ST (↑)
CopulaGAN	8.53%	16.75%	49.58%	0.60
GaussianCopula	12.41%	19.24%	**50.23%**	0.18
CopulaKDE	7.39%	14.14%	53.00%	0.76
GaussianKDECopula (8,461s)	8.30%	8.84%	49.28%	0.89
CopulaDiff	2.10%	4.61%	50.34%	0.86
SimpleKDE	1.98%	4.64%	62.89%	0.90
TabKDE	**1.56%**	**4.51%**	62.23%	**0.92**

Default	Marginal Err. (↓)	Pairwise Corr. (↓)	DCR (→ 50)	C2ST (↑)
CopulaGAN	11.50%	21.13%	52.98%	0.74
GaussianCopula	12.33%	21.90%	**49.59%**	0.41
CopulaKDE	8.99%	12.48%	56.36%	0.58
GaussianKDECopula (9,239s)	7.02%	7.58%	50.41%	0.95
CopulaDiff	**1.47%**	**3.29%**	50.96%	**0.98**
SimpleKDE	3.33%	5.16%	66.05%	0.87
TabKDE	1.55%	9.93%	63.46%	0.96

Magic	Marginal Err. (↓)	Pairwise Corr. (↓)	DCR (→ 50)	C2ST (↑)
CopulaGAN	10.21%	9.03%	51.23%	0.66
GaussianCopula	11.19%	6.34%	**50.10%**	0.51
CopulaKDE	11.42%	7.20%	55.40%	0.73
GaussianKDECopula (1,477s)	2.30%	5.00%	50.22%	**0.99**
CopulaDiff	0.94%	**1.72%**	52.03%	0.94
SimpleKDE	3.12%	3.30%	62.62%	0.97
TabKDE	**0.78%**	2.72%	63.02%	0.94

Beijing	Marginal Err. (↓)	Pairwise Corr. (↓)	DCR (→ 50)	C2ST (↑)
CopulaGAN	7.79%	12.11%	50.89%	0.78
GaussianCopula	10.01%	6.00%	**50.05%**	0.11
CopulaKDE	12.04%	17.07%	53.94%	0.74
GaussianKDECopula (9,288s)	2.69%	6.56%	50.66%	**0.99**
CopulaDiff	2.13%	4.50%	50.29%	0.96
SimpleKDE	2.06%	4.68%	55.45%	0.94
TabKDE	**1.37%**	**3.74%**	54.24%	0.95

Table 30: TabKDE vs Copula+KDE Baselines.

DP Gaussian Copula (Adult)	Marginal Err. (↓)	Pairwise Corr. (↓)	DCR (→ 50)	C2ST (↑)
$\epsilon = 0.1$	18.44%	32.56%	49.88%	0.37
$\epsilon = 1$	16.72%	29.04%	50.12%	0.36
$\epsilon = 5$	16.27%	28.69%	49.97%	0.37
$\epsilon = 10$	16.92%	27.76%	49.75%	0.33
$\epsilon = 100$	17.46%	29.80%	49.80%	0.29

Table 31: DP Gaussian Copula on Adult with different privacy budget ϵ (smaller implies stronger privacy).